Report on DLR-JAXA Joint Experiment

The Kirari Optical Downlink to Oberpfaffenhofen (KIODO)

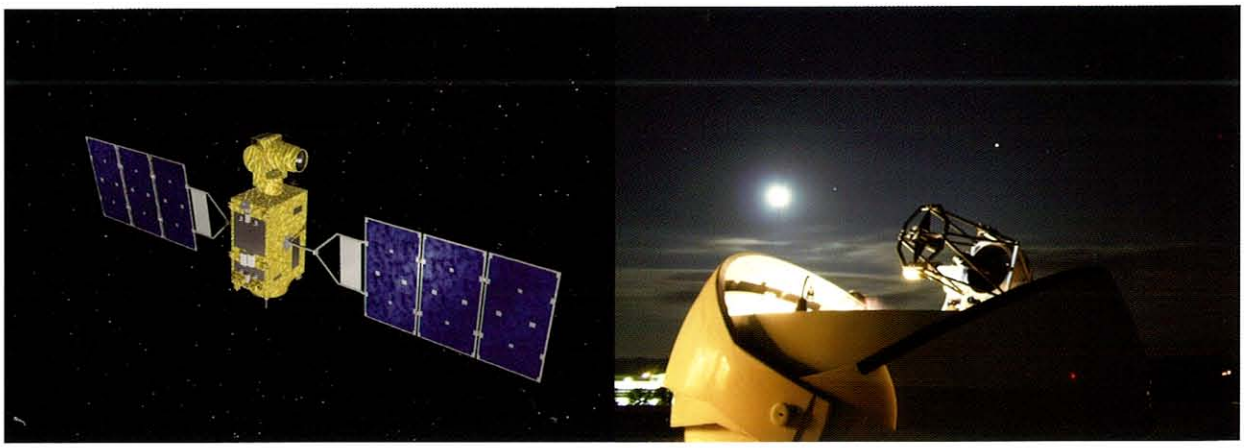

April 2007

Table of contents

1 Introduction

Japan Aerospace Exploration Agency (JAXA) had built and launched the Optical Inter-orbit Communications Engineering Test Satellite (OICETS) with the optical terminal called the Laser Utilization Communications Equipment (LUCE) and performed optical communication tests with ESA's Advanced Relay and Technology Mission (ARTEMIS) satellite around the end of 2005. OICETS' communications technology is mostly compatible to the optical ground station which was built by German Aerospace Center (DLR) for communications tests in the ongoing projects CAPANINA and TerraSAR-LCT-IOV. Therefore, DLR and JAXA would like to execute a downlink experiment from OICETS to DLR's optical ground station. Purpose of this experiment was to demonstrate the feasibility of high-speed optical data downlinks from LEO (e.g. earth-observation) satellites to simple, inexpensive optical ground terminals for future use.

The cooperative project was named as "the Kirari Optical Downlink to Oberpfaffenhofen (KIODO)." DLR and JAXA entered into Joint Research Agreement on the date of the last signature, 28th April, 2006. The Joint Research Agreement remains effective until 31st December 2006.

The first meeting was held on 14th Feb 2006 at DLR Oberpfaffenhofen, Wessling, Germany. The second meeting was on 26th April 2006 at JAXA Tsukuba Space Center, Japan. In those meetings, the period of experiments was determined from 7th June to 30th June 2006. The KIODO trials were successfully conducted during that period, and the third meeting was held on 5th and 6th Dec. 2006 at DLR Oberpfaffenhofen to discuss the results.

This document describes the objectives of KIODO project, introductions of the facilities, experiment scenarios, and interface controls through the section 2 to the section 5. In the section 6, the results of feasibility assessments are summarized. The section 7 shows the schedule. The experimental conditions and measured data in each trial are given in the section 8. The results are summarized in the section 9 and the detailed discussions on some issues are described in the section 10.

2 Objectives

The purpose of KIODO was to demonstrate the feasibility of high-speed optical data downlinks from OICETS to simple, inexpensive optical ground terminals for future use, and objectives are listed below.

- To derive data on the downlink transmission channel with high angular velocities in optical terminals' movement under the atmospheric effects.
- To obtain criteria for investigating the atmospheric influences.
- To measure the received power fluctuations on the uplink and downlink channels.
- To measure Bit Error Rate (BER) of the received digital signal on the downlink channel.
- To evaluate pointing accuracy of optical terminals.
- To evaluate accuracy of acquisition and tracking performance of optical terminals.

3 Facilities

3.1 Major characteristics of OICETS and LUCE

OICETS is a relatively small satellite with a mass of approximately 570 kg. The schematic drawing is shown in Figure 3.1-1. It was launched by a Dnepr Launch Vehicle from the Baikonur Cosmodrome in the Republic of Kazakhstan. The orbit is circular at the altitude of 610 km with the inclination of 97.8 degrees. The major characteristics of OICETS are given in Table 3.1-1 [JON06].

LUCE shown in Fig. 3.1-2 is equipped on the satellite as a mission payload to demonstrate the inter-orbit laser communications. The terminal consists of two separated parts, the optical and electrical parts. The optical part involves an optical antenna mounted on two axes gimbals and the inner optical setup shown in Fig. 3.1-3. The optical antenna is a center-feed Cassegrain mirror-type telescope and attached to the anti-earth side of the satellite. The electrical part is put in the satellite body and provides functions to control the acquisition, tracking and pointing mechanisms as well as the communication electronics. Table 3.1-2 describes the major performances of LUCE.

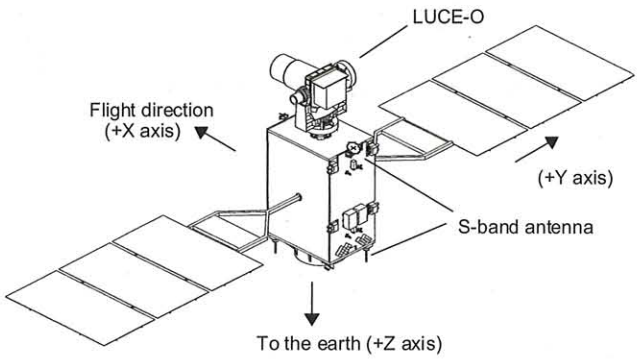

Figure 3.1-1 On-orbit satellite configuration of OICETS.

Figure 3.1-2 Overview of the LUCE optical part (right) and the LUCE electrical part (left).

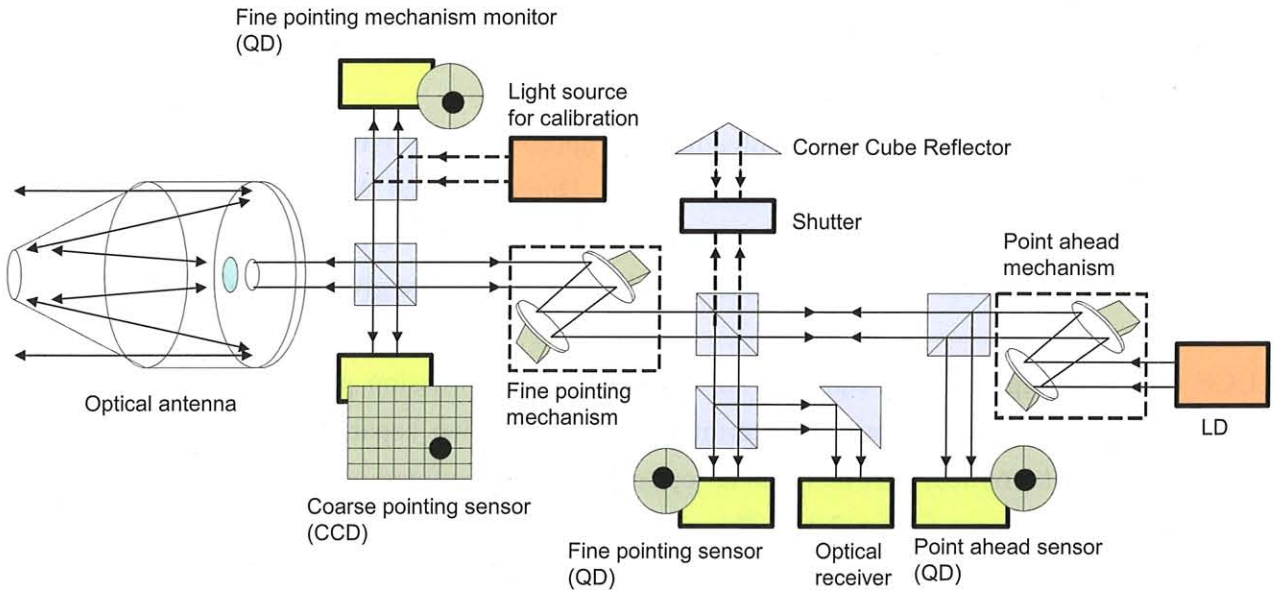

Figure 3.1-3 Optical setup of LUCE-O

Table 3.1-1 Major characteristics of OICETS

ITEM	VALUE
Launch Date	23rd Aug. 2005
Launch site	Baikonur Cosmodrome in the Republic of Kazakhstan.
Eccentricity	0
Attitude control	Three-axis stabilized
Size	9.4 m× 1.8m ×3.1 m
Orbit inclination	97.8 deg
Weight	570 kg

Table 3.1-2 Major characteristics of LUCE

ITEM	VALUE
Weight	Approx. 140 kg
Power	Approx. 220 W (during communication)
Optical antenna	
Structure	Cassegrain-type telescope
Wavefront error	Less than $\lambda/20$ rms within 1 mrad field of view (λ=847 nm)
Magnification	x 20
Effective diameter	26 cm
Transmitting laser beam	
Maximum laser power	100 mW (modulated mean value)
Emitted intensity	280–780 MW/sr
Full beam diameter	($1/e^2$) 120 mm
Full beam divergence angle	(FWHM) Approx. 5.5 μrad
Wavelength	LD1: 848 nm, LD2: 847 nm (nominal)
Optical receiver	
Device	Si-APD detector
BER performance	10^{-6} at −71.4 dBm
Coarse-pointing mechanism	
Structure	Two-axis gimbals (azimuth and elevation mount)
Angular coverage	Az : − 10~370 deg. El: 0–120 deg.
Actuator	Direct drive motors
Tracking accuracy	±0.01 deg.
Optical sensor	Si-CCD
Field of view	±0.2 deg.
Fine-pointing mechanism	
Structure	A pair of independent one-axis moving mirrors
Angular coverage	±500 μrad.
Actuator	Multi-layered piezo-electric actuators
Tracking accuracy	±0.92 μrad. (acquisition), ±0.64 μrad. (communication)
Optical sensor	Si-Quadrant detector
Field of view	±200 μrad.
Point-ahead mechanism	
Structure	A pair of independent one-axis moving mirrors
Angular coverage	±75 μrad.
Actuator	Multi-layered piezo-electric actuators
Point-ahead accuracy	±1.58 μrad (acquisition), ±1.85 μrad (communication)
Optical sensor	Si-Quadrant detector

3.2 Major characteristics of the Optical Ground Station

3.2.1 Geographical Location

DLR's Institute for Communication and Navigation is located in Oberpfaffenhofen (OP) in the Argelsrieder Feld. The optical ground station (OGS-OP) is located on the roof of the institute's building. The coordinates of the optical ground station are:

OGS-OP: 48°04'55.72° N, 11°16'31.77° E

The portion of the sky viewed by OGS-OP is depicted in Figure 3.2.1-1 with respect to azimuth and elevation angles.

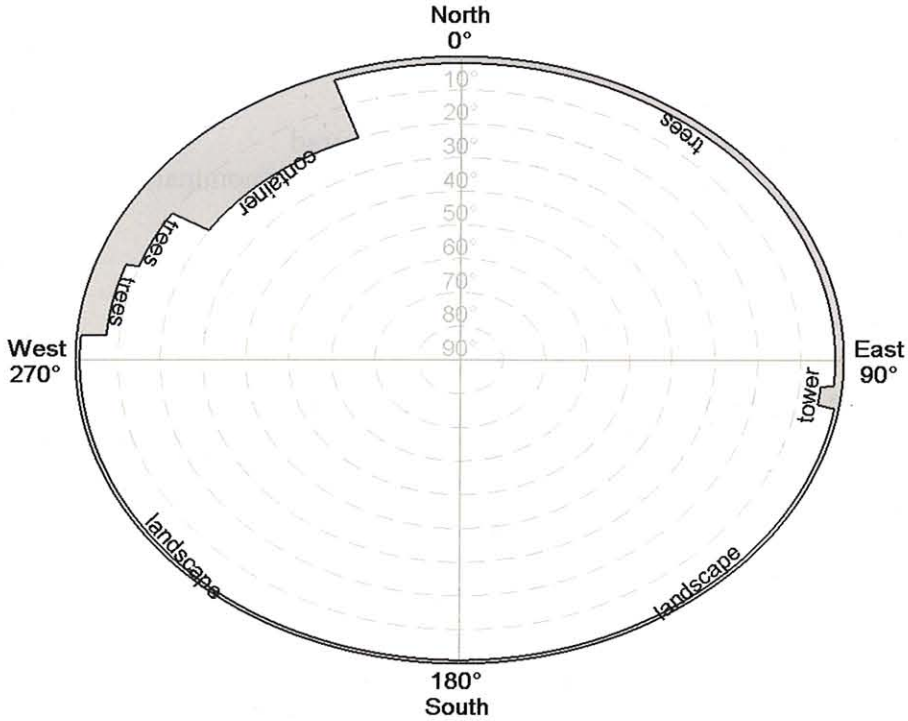

Figure 3.2.1-1 Sky view of the OGS-OP.

3.2.2 Dome, Mount and Telescope

The OGS consists of a clamshell dome having a diameter of 4 m. The dome can be seen in Figure 3.2.2-1. In the middle of the dome, an Astrophysics mount supports the 40-cm cassegrain telescope. This terminal is transportable and can be seen in Figure 3.2.2-2 and Figure 3.2.2-3.

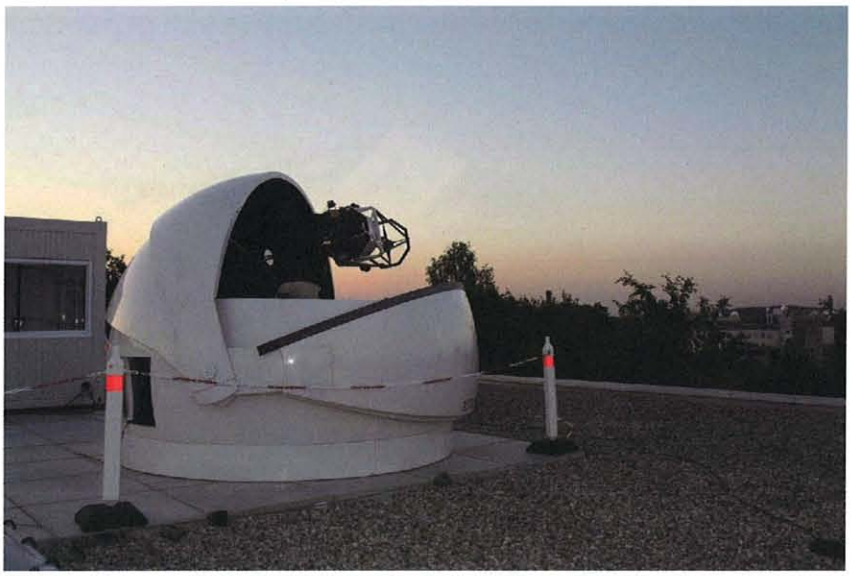

Figure 3.2.2-1 DOME of the OGS on the building's roof.

Figure 3.2.2-2 Front view of the 40-cm telescope.

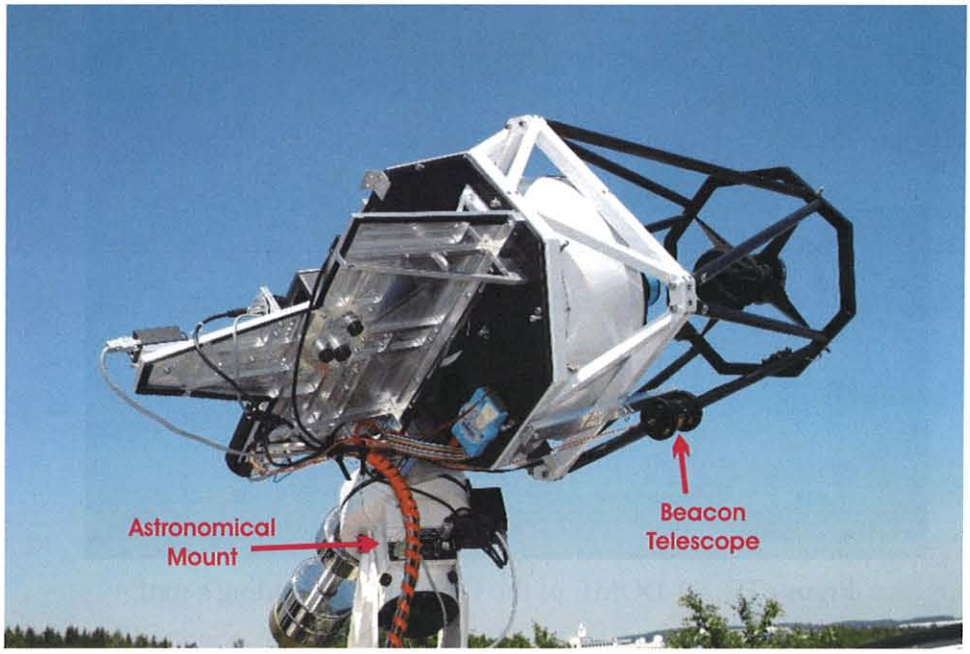

Figure 3.2.2-3 Rear view of the 40-cm telescope.

3.2.3 Tracking Capability

The acquisition of the target is a two-step process. First, the telescope is pointed at the target open-loop and based on orbit data only, i.e. without visual feed-back. The system is designed to be accurate enough to illuminate the target with its beacons and to get the target into the camera's FOV. Next, the target is acquired on the acquisition (wide FOV) and tracking camera (narrow FOV), and the closed-loop tracking keeps the target centered in the FOV with high accuracy (<100μrad), so that an uninterrupted communication is ensured.

Note that the mount must be calibrated shortly before each trial in order to keep the pointing accuracy high enough.

3.2.4 OGS Beacons

Two beacons were transmitted from the 40-cm telescope with a divergence angle of approximately 5 mrad. The beacons were multimode beams coming out of two 400-μm multimode fibers. Two 5-cm beacon telescopes were mounted on the 40-cm telescope with a separation distance of about 50 cm. Characteristics of the beacons are given in Table 3.2.4-1.

Table 3.2.4-1

	Beacon 1	**Beacon 2**
Emission Central Wavelength	807.8 nm	809.1 nm
Emission FWHM	2.0 nm	3.7 nm
Max. Output power	8.5 W	9.5 W
Percentage of total power	50 %	50 %

3.2.5 Optical Instruments

Overview

The communication receiver, the tracking camera, the measurement cameras and a powermeter are located on a metal plate fixed behind the telescope (see Figure 3.2.5-1). The optical system is depicted in Figure 3.2.5-2. Measurement data are stored on Windows computers with time stamps. UTC time is obtained from a GPS receiver and delivered to each computer. UTC time is delivered to each computer by the use of IRIG (Inter-rang instrumentation group) PCI cards.

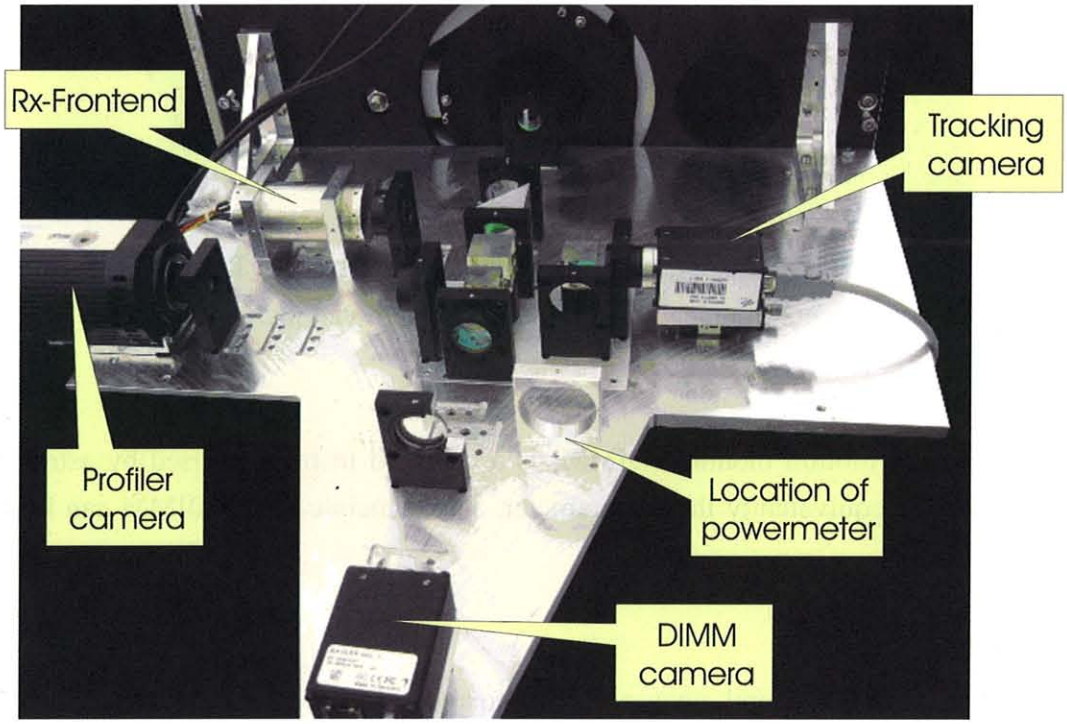

Figure 3.2.5-1 Optical System behind the 40-cm telescope

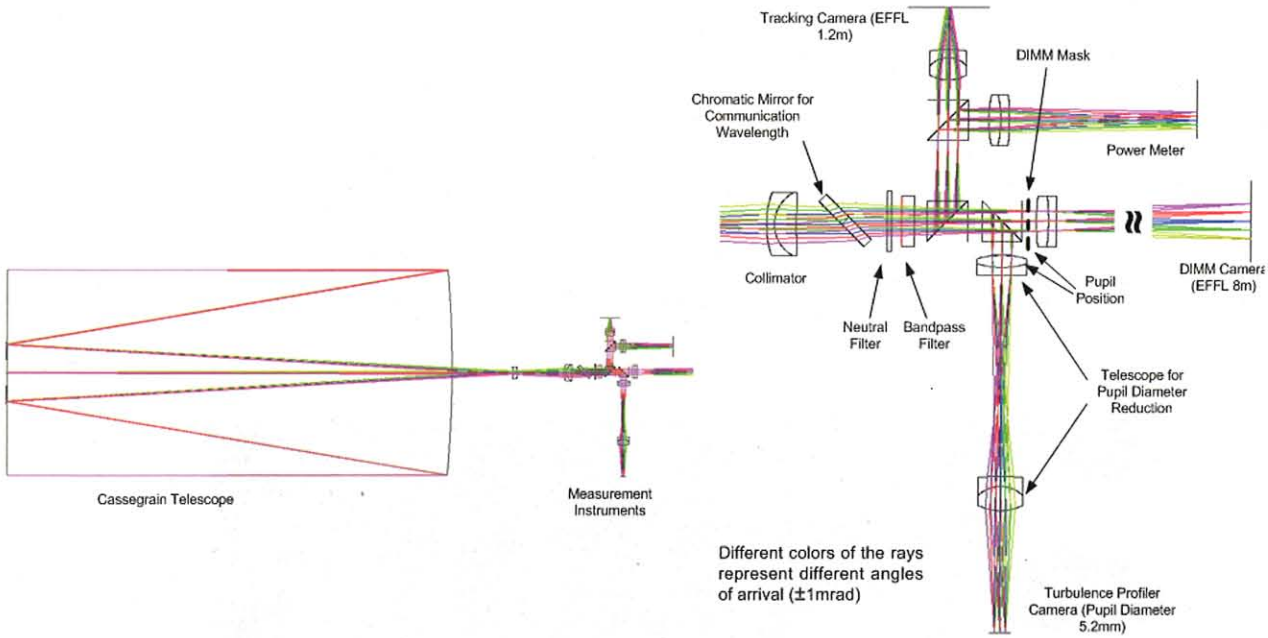

Figure 3.2.5-2 Description of the optical system behind the telescope. The optical "arm" of the communication receiver is here not visible.

DIMM

The differential image motion monitor (DIMM) is a standard instrument used by astronomers to measure the seeing or equivalently the r_0 parameter. The principle of the DIMM can be found in [SAR90]

Profiler Camera (Scintillation)

The profiler camera records pupil images. These images are used to estimate scintillation and turbulence parameters. Turbulence along the path can be retrieved from using weak-fluctuation theory as described in [TOK02]. Because the KIODO trials are mostly under the strong-fluctuation regime, the calculated turbulence profile will be shown only for the highest elevation of the trial where the fluctuations are the weakest.

Powermeter

The powermeter consists of a PIN diode with a large detector size.

Rx-Front-End

The communication detector consists of an avalanche photodiode (APD) with a diameter of 1.5 mm. The receiver performance curve as measured in the lab (after the KIODO experiment) is shown in Figure 3.2.5-3. The abscissa of this curve is the power impinging on the APD. The components of the receiving front-end used during KIODO are shown in Figure 3.2.5-4. For all trials, the BER was estimated twice per second, this gives a BER resolution of 4×10^{-8}.

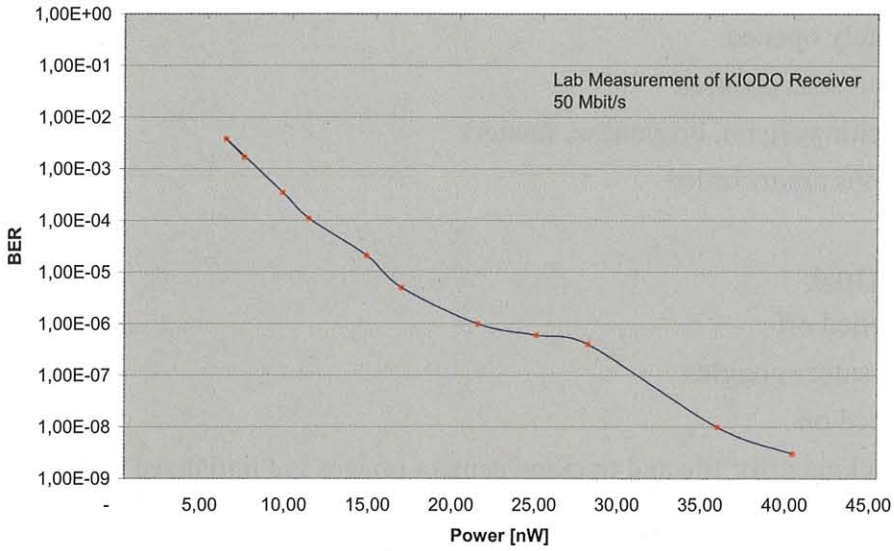

Figure 3.2.5-3 Lab performance curve of the KIODO receiver at 50 Mbit/s.

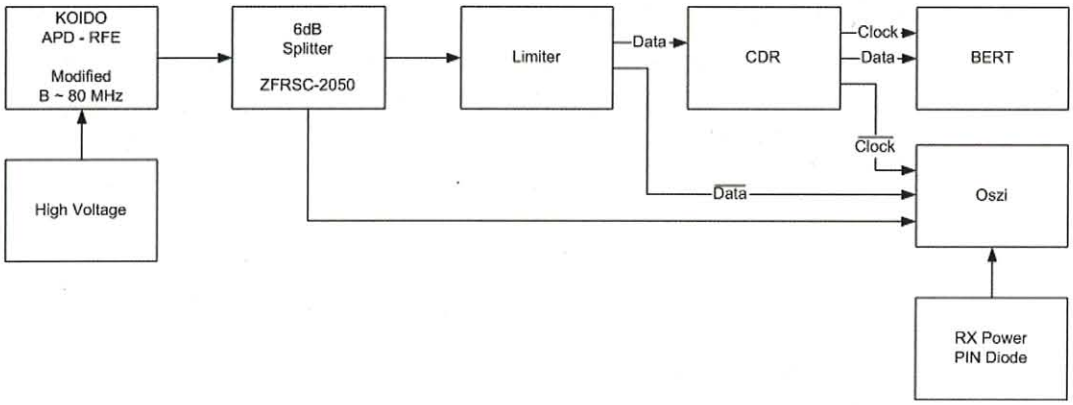

Figure 3.2.5-4 Typical frontend configuration used for KIODO (depending on the KIODO trials, the configuration may slightly vary). RFE = Receiver Front-End, CDR = Clock/Data Recovery, BERT = Bit-error-rate tester, Oszi = Oscilloscope.

3.2.6 Preparation of OGS before link trial

A few hours before trial:

- The Rx-front-end is tested over a 400-m test range.
- Computers and softwares are started
- Camera and optical components are adjusted if necessary
- Orbit data are loaded on tracking computer
- The mount is calibrated by known stars (if clouds, backup = reference terrestrial source)

10 minutes before trial:

- Experiment area is secured (eye-safety)
- Check that nothing obstructs telescope motion
- Dome is completely opened
- Move telescope to start position
- Check camera settings (gain, brightness, shutter)
- Weather conditions are recorded

<u>30 seconds before trial:</u>
- All lamps are turned off
- Everyone wears safety goggles
- Beacons are turned on
- Recording of tracking error file and tracking camera images are initialized

3.3 Experiment systems

The operation system for experiments is shown in Fig. 3.3-1. OICETS employs S-band frequency ranges for communications with the ground network facilities. In the figure, the HSB stands for a high speed S-band down link of 1Mbps data rate which is used to send the OICETS mission telemetries to a ground facility. The USB indicates the unified S-band employed to transmit operation commands from the ground stations to OICETS. The USB is also used to send telemetries from the satellite to the ground stations. OICETS is connected to the OGS with the optical downlink at 50 Mbps.

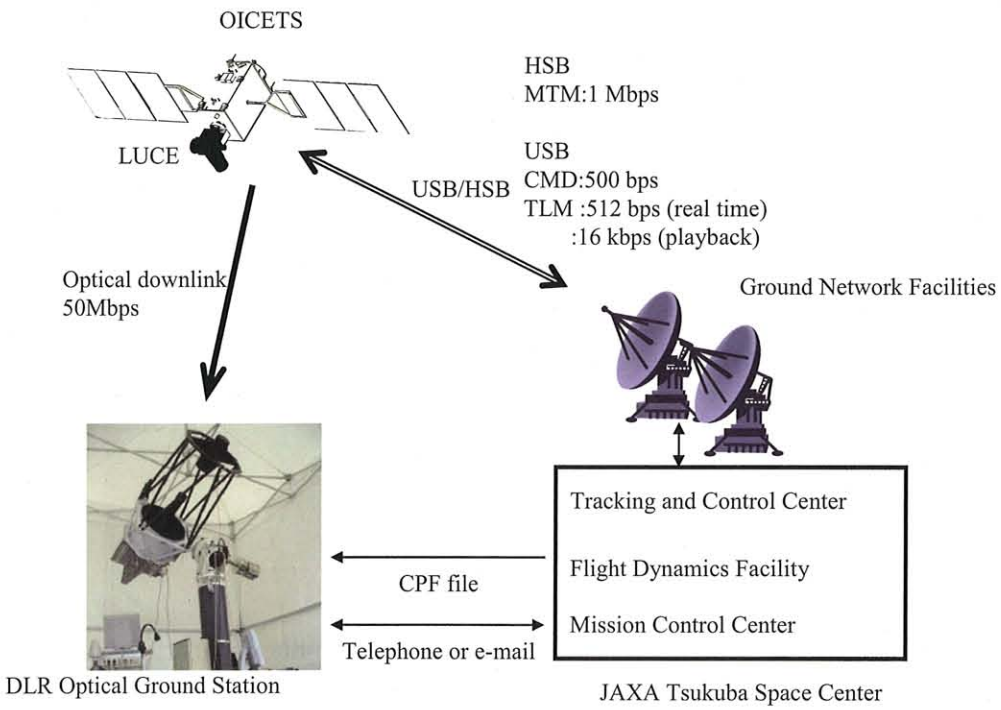

Figure 3.3-1 Operation systems for experiments

4 Scenario

4.1 Attitude controls

Prior to the ground-satellite trials, the attitude control system of OICETS should be set in the Inertia Reference Mode (IRM) to fix the satellite attitude on the inertia space as shown in Fig. 4.1-1. The revolution around the earth with this fixed attitude enables LUCE to point the earth surface. In this figure, p_0 indicates the position at which OICETS moves into the IRM. At the position p_1, LUCE starts to point the optical antenna toward the OGS with open-loop control. OICETS and the OGS establish the optical link at p_2, keep the link during p_3. The link is vanished at the position p_4. In the KIODO trials, OICETS appeared in the north sky of the OGS and headed the south sky.

In the IRM, the rotational velocities of reaction wheels are controlled to reduce the difference between the expected and measured attitudes. When OICETS's attitude is set in a normal mode, both the sun and earth sensors are used as well as the Inertia Reference Unit (IRU). The outputs of these sensors are employed to compensate the measurement error of the IRU. However, in the IRM, both the sun and earth sensors become invalid. Therefore, some preparative information should be given to OICETS for a proper compensation of the IRU measurement error. As a result, three procedures are required for the experiments. The first step is to perform the IRM prior to the experiment and evaluate the error in the IRU measurement by referring to the sensors' outputs. The evaluated IRU error is used to create information for compensation. The second step is to set the satellite attitude back to the normal mode and provide the compensatory information to OICETS. The third step is to carry out the IRM again to establish the optical link with the OGS.

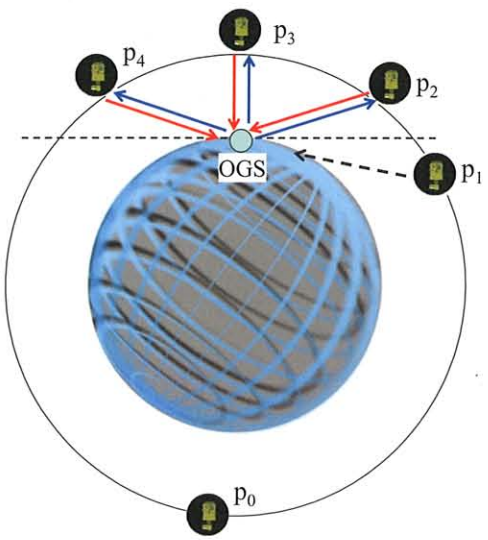

Figure 4.1-1 Inertia Reference Mode (IRM).

4.2 Sequences to establish an optical link

The sequences to establish an optical link between the OGS and OICETS are shown in Figs. 4.2-1, where the OICETS is already set into the IRM attitude. Fig. 4.2-1(a) indicates the first step to establish the optical link. Optical antennas in both terminals point to each other by open-loop control, and the OGS emits the beacon beam toward a predicted direction of OICETS. Fig. 4.2-1(b) shows the second step where OICETS emits the communication beam toward the OGS upon the detection of the beacon beam. In the third step, the mutual illumination is kept as described in Fig. 4.2-1(c) until the end of the scheduled experiment periods.

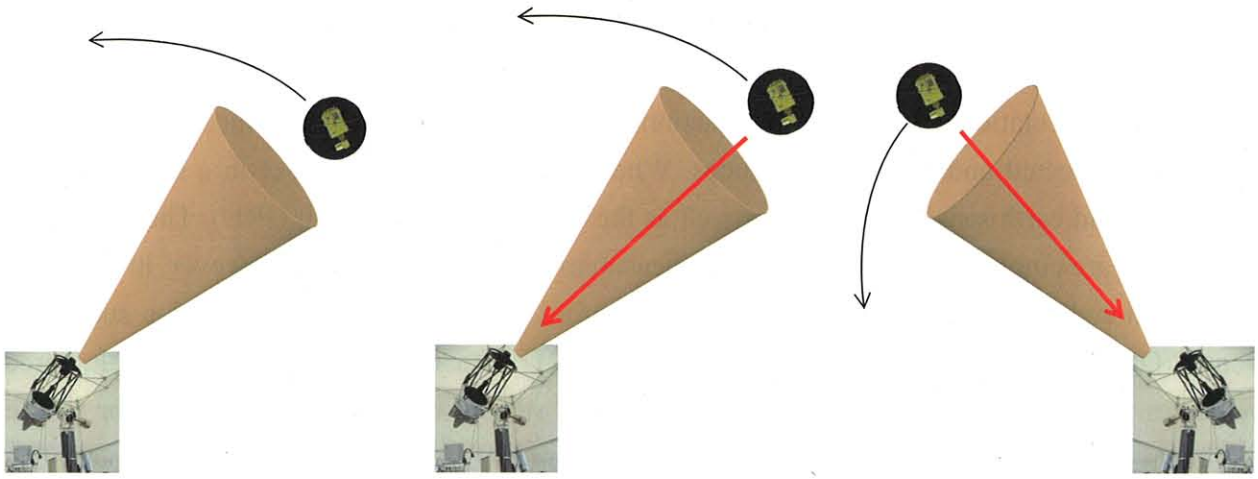

(a) (b) (c)

Figure 4.2-1 Procedures for optical communication. (a) OGS emits the beacon beam. (b) OICETS sends out the communication beam toward the OGS. (c) The OGS and OICETS keep mutual illumination.

5 Interface control

5.1 Optical interface

OICETS uses the Non Return to Zero (NRZ) format at 49.3724 Mbits/sec in its down link. The required irradiance of a beacon illuminating OICETS for proper coarse pointing is independent on the polarization and supposed to be 2~58 nW/m^2 for the wavelength ranges of 797~808nm and 815~825nm. When OICETS terminal detects the beacon light transmitted by the OGS, OICETS transmits the signal beam of the wavelength of 843nm~853nm, the left-handed circular polarization, and the intensity of $85*10^6$W/sr~$780*10^6$W/sr.

5.2 Orbit information

JAXA employed the Range and Range Rate (RARR) using radio-frequency range for the OICETS orbit determination and prediction. JAXA provided the orbit prediction files in the Consolidated Prediction Format (CPF) [RIC06,PEA02] to DLR. The accuracy of CPF files would be about a few dozen meters because of the orbit determination accuracy by the RARR and low solar activities at that time.

6 Feasibility assessments

6.1 Optical link

Table 6.1-1 and Table 6.1-2 show the link budget calculations for the downlink. An elevation angle of 10° is considered. Losses are given here as linear factors. Figure 6.1-1 shows how the power has been decreased with the elevation in order to keep constant the mean optical power on the LUCE terminal. The clear-sky extinction coefficient was evaluated as a function of altitude for a wavelength λ = 810 nm ([MAY02] has been used). A theoretical calculation of the uplink scintillation based on a spherical wave is shown in Figure 6.1-2

Table 6.1-1 Downlink power budget

Downlink		
Scenario parameters	**Values**	
Laser Power	0.10	W
Wavelength	8.47E-07	m
Tx Divergence Angle (FWHM)	5.50E-06	rad
Link Distance L	2.00E+06	m
Rx intensity spot radius (1/e2)	9.34E+00	m
Pointing Loss	0.50	
Atmospheric Attenuation	0.19	
Scintill. Loss (Beam Spread)	0.83	
Mean Rx-Intensity	7.23E-04	W/m2
Rx Aperture (Diameter)	4.00E-01	m
Rx Optical Loss	0.6	
Scintill. Loss (Fluctuations)	0.10	
Pointing Loss (Fluctuations)	0.50	
Minimum Received Power	**1.98E-07**	**W**

Table 6.1-2 Link margins of ground detectors

Detector	Communication	Tracking	Powermeter	DIMM	Profiler	
% of Received Power	8	4	4	42	42	
Required Power	7.06E-08	2.29E-11	1.00E-9	5.54E-08	4.32E-08	**W**
Link Margin	4.5	39.4	15.8	5.5	6.6	**dB**

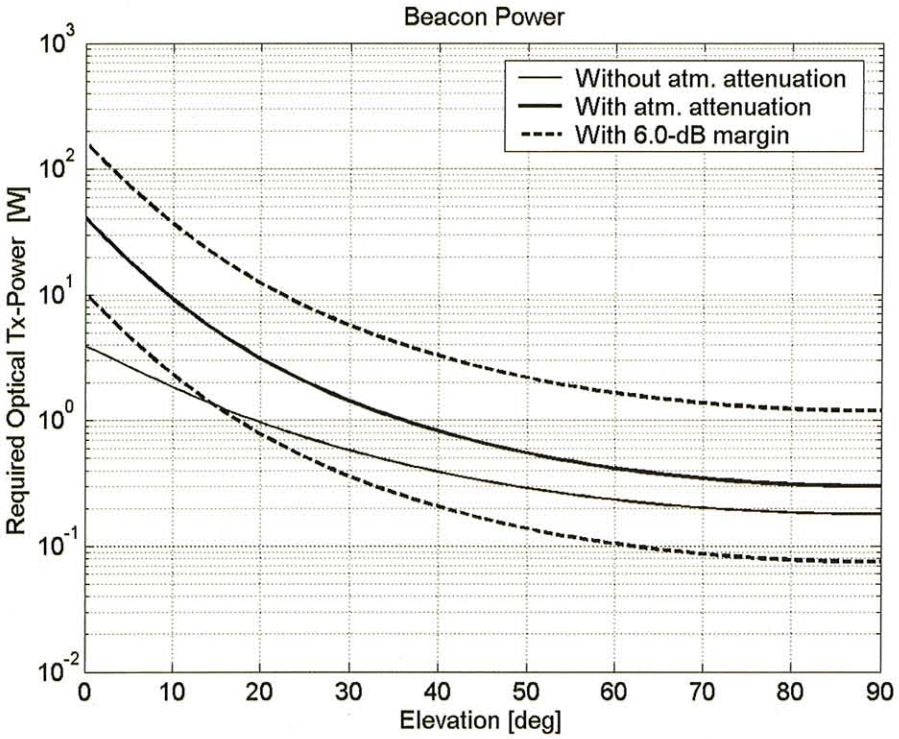

Figure 6.1-1 Level of the total optical output power that the beacon should transmit in order to obtain a constant and proper power level on OICETS.

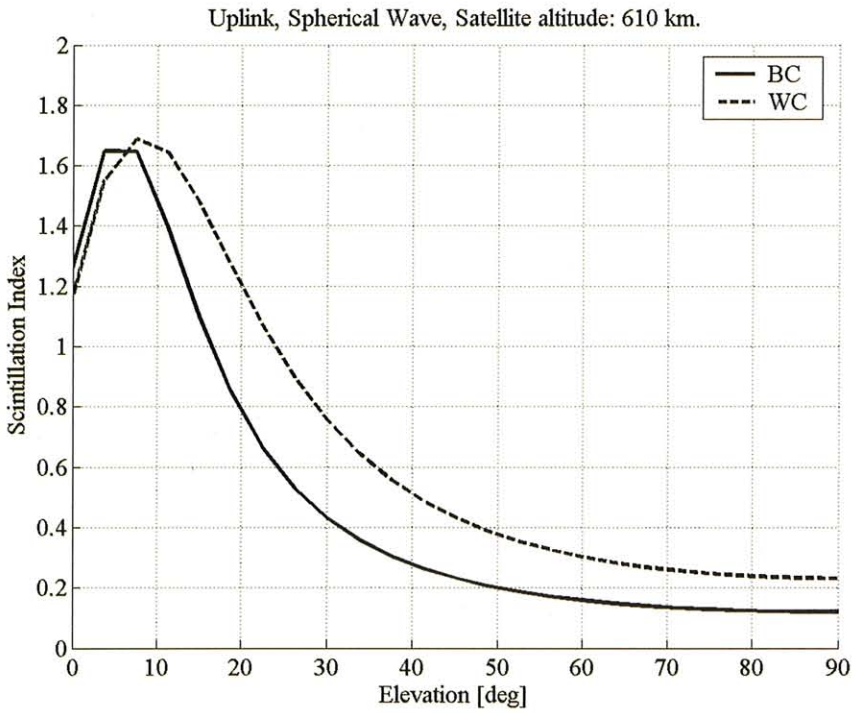

Figure 6.1-2 Scintillation index for the uplink calculated from [AND05] using the spherical-wave assumption. The atmospheric turbulence (C_n^2) follows the Hufnagel-Valley model. Best and worst turbulence cases are displayed.

6.2 Satellite operation

Figure 6.2-1 is a sample computation result to determine available experiment periods for the experiment on 21st Jun, 2006. For such a computation, the elevation angle of the DLR's ground station (larger than 10 degs. for the first 3 trials and 0 deg. for the rest) and the elevation angle of LUCE (larger than 7 degs.) are taken into consideration. In the figure, we extracted two pass windows because we were able to expect a slow angular movement on LUCE gimbal's operation and to avoid the influence of the sun light. As a results, the trial period for Experiment (1) was 2min 30sec and for Experiment (2) was 1min 50sec. We repeated the similar procedures to fine potential pass windows for all the trials. The results in each trial are described in Sec. 8.

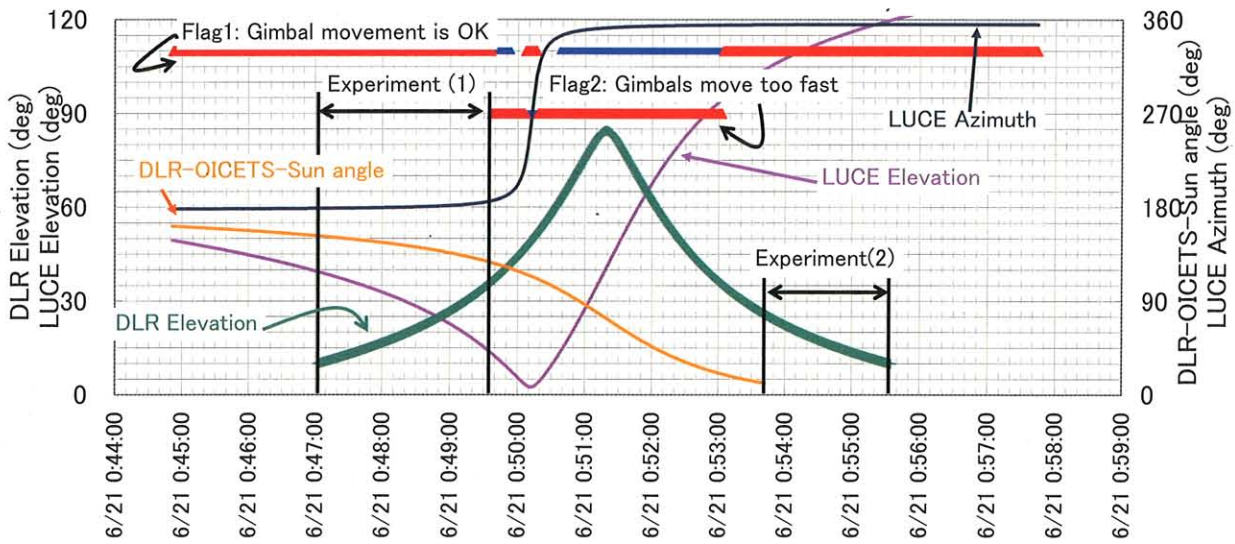

Figure 6.2-1 Sample computation for planning of experiment.

6.3 Others

The laser ranging was forbidden in the period of KIODO experiments.

7 Schedule

The experiment calendar is shown in Fig. 7-1. The notation "V" indicates the experiment and "O" means that OICETS is put into the inertia reference mode to obtain the measurement error of the IRU. The asterisk (*) neighboring to "V" tells that the link was not established due to the whether conditions.

June, 2006

5	6	7	8	9	10	11
Mon	Tue	Wed	Thu	Fri	Sat	Sun
		V 01:13 - 01:16		V 00:02 - 00:05		
O		O				

12	13	14	15	16	17	18
Mon	Tue	Wed	Thu	Fri	Sat	Sun
		V 01:04 - 01:07	V 23:51 - 23:57			

19	20	21	22	23	24	25
Mon	Tue	Wed	Thu	Fri	Sat	Sun
		V(*) 00:54 - 00:59		V(*) 01:19 - 01:24		
O		O				

26	27	28	29	30
Mon	Tue	Wed	Thu	Fri
		V 00:46 - 00:51		V(*) 01:11 - 01:16

Figure 7-1 Experiment calendar. "V" indicates the date of experiments and "O" means to carry out the measurement of IRU error. The asterisk (*) means that the link could not be established.

8 Results of each trial

8.1 Trial Overview

1	7th June	1E-5 – Too long Exposures for Cameras
2	9th June	Signal received – No Communication
3	14th June	1E-5
4	16th June	1E-5
5	21st June	Cloudy – OICETS did not see OGS-OP
6	23rd June	Cloudy, rainy – OICETS did not see OGS-OP
7	28th June	1E-6
8	30th June	Cloudy – OICETS did not see OGS-OP

8.2 First trial on 7th June, 2006

8.2.1 Configuration and predictions

KIODO Experiment Configuration Sheet

Revision: 1
Date: 2006/6/6

Experiment date:	7th June 2006
Planning Time (UT)	01:13:08 - 01:16:09
Test Objective	Downlink

S/C: OICETS

No.	Parameter	Setting	Note
1	LD 1 or 2	LD1	nominal case: 1
2	LD modulation mode (PN or CW)	PN	
3	LD output power (100mW or 80mW)	100mW	

DLR Ground station

No.	Parameter	Setting	Note
1	Wavelength	809 nm	
2	Total Beacon Power	0.3 W	at 90° elevation
3	Divergence angle	5 mrad	FWHM
4	Power percentage for beacons	50, 50	beacons at 809 nm
5	Mode of beacon power	adjustable	
6	Power percentage for instruments	8, 23, 23, 23, 23	Rx, Tracking, Profiler, DIMM, Powermeter
7			

Figure 8.2.1-1 Configuration sheet.

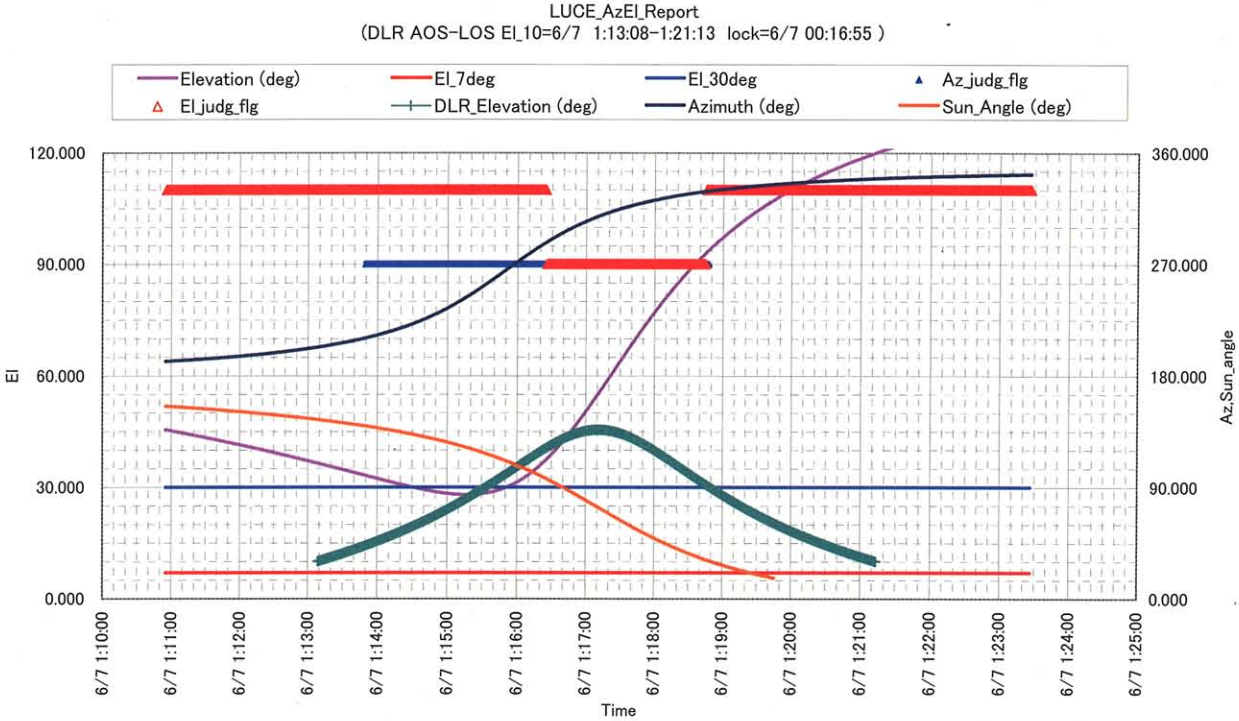

Figure 8.2.1-2 Predictions on angular movements of OGS and LUCE

8.2.2 OGS measurement

For the first trial, less optical power was expected by DLR. As a result, instrument cameras have saturated and measurement data could not be exploited.

Weather at OGS-OP during experiment: clear sky with thin clouds, 8°C

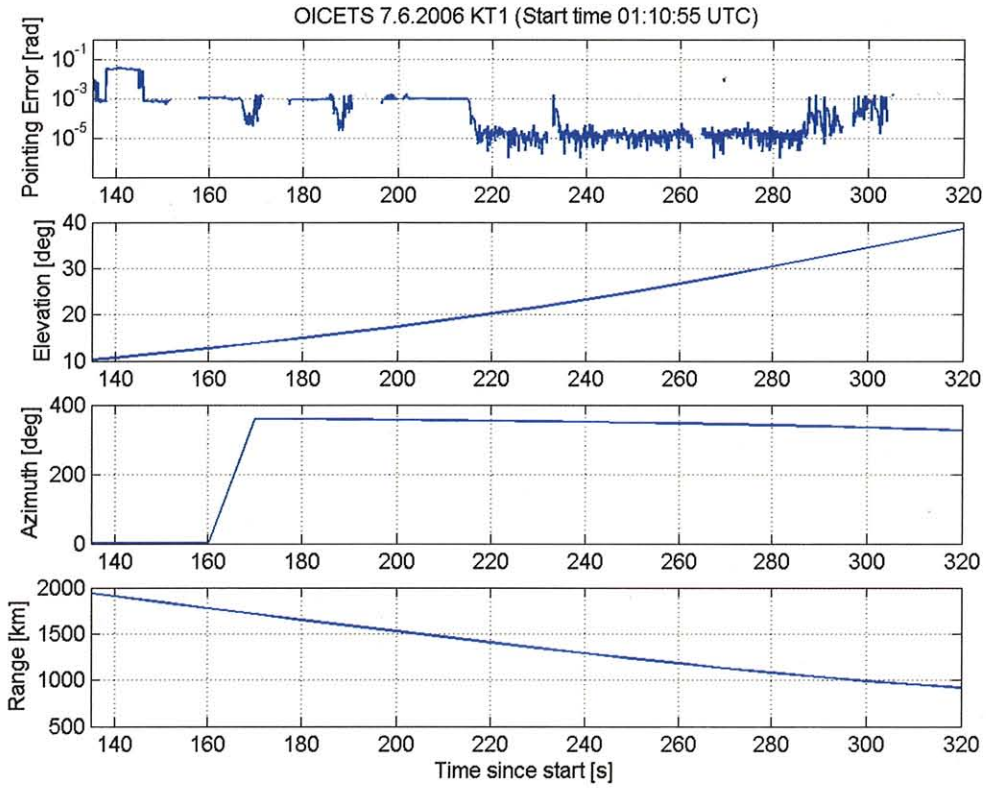

Figure 8.2.2-1 Pointing error of OGS-OP along with link parameters for Trial #1.

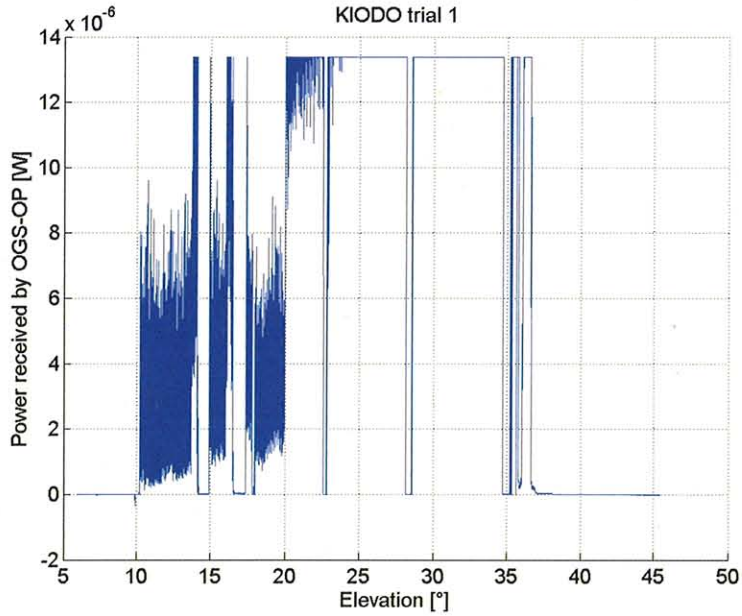

Figure 8.2.2-2 Optical Power impinging on 40-cm telescope in Trial #1 (Values measured by PIN diode in optical system in calculated back to power in aperture). There is however saturation.

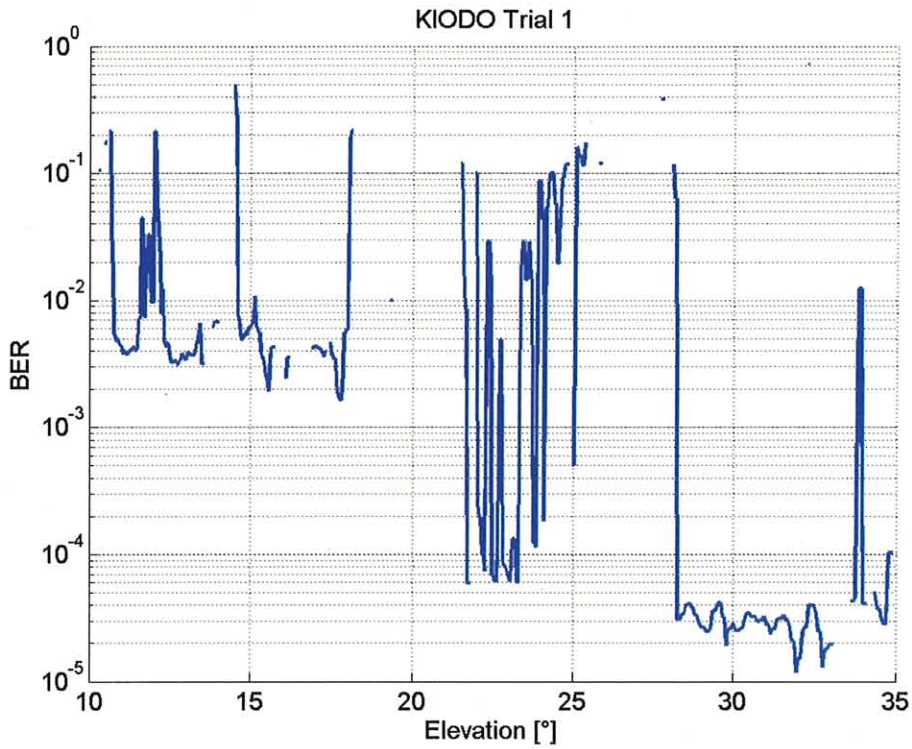

Figure 8.2.2-3 Bit error rate of Trial #1.

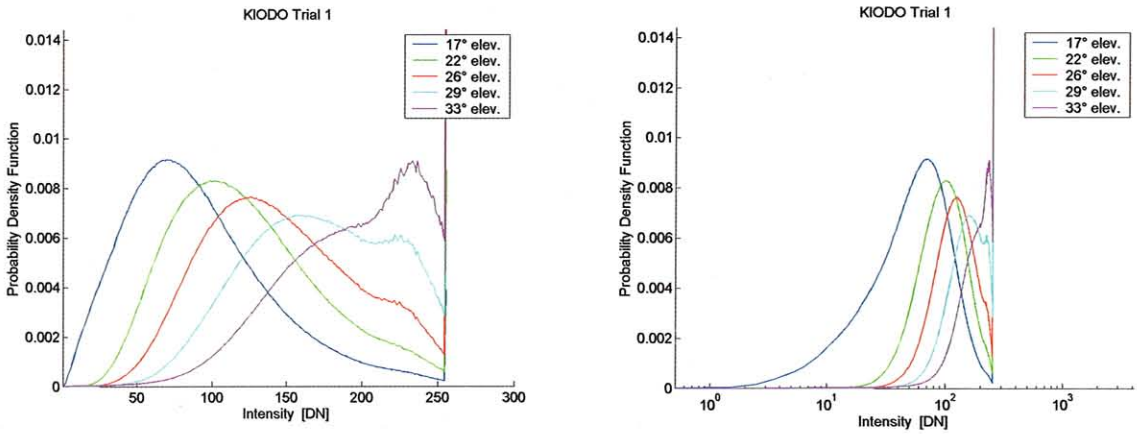

Linear scale Logarithmic scale

Figure 8.2.2-4 PDF of the intensity for Trial #1. The intensity corresponds to the pixel value of the profiler camera (DN = Digital Number)

8.2.3 OICETS measurement

The coarse pointing sensor detected the beacon light from the OGS around 01:12:48, and the acquisition time was 75 msec.

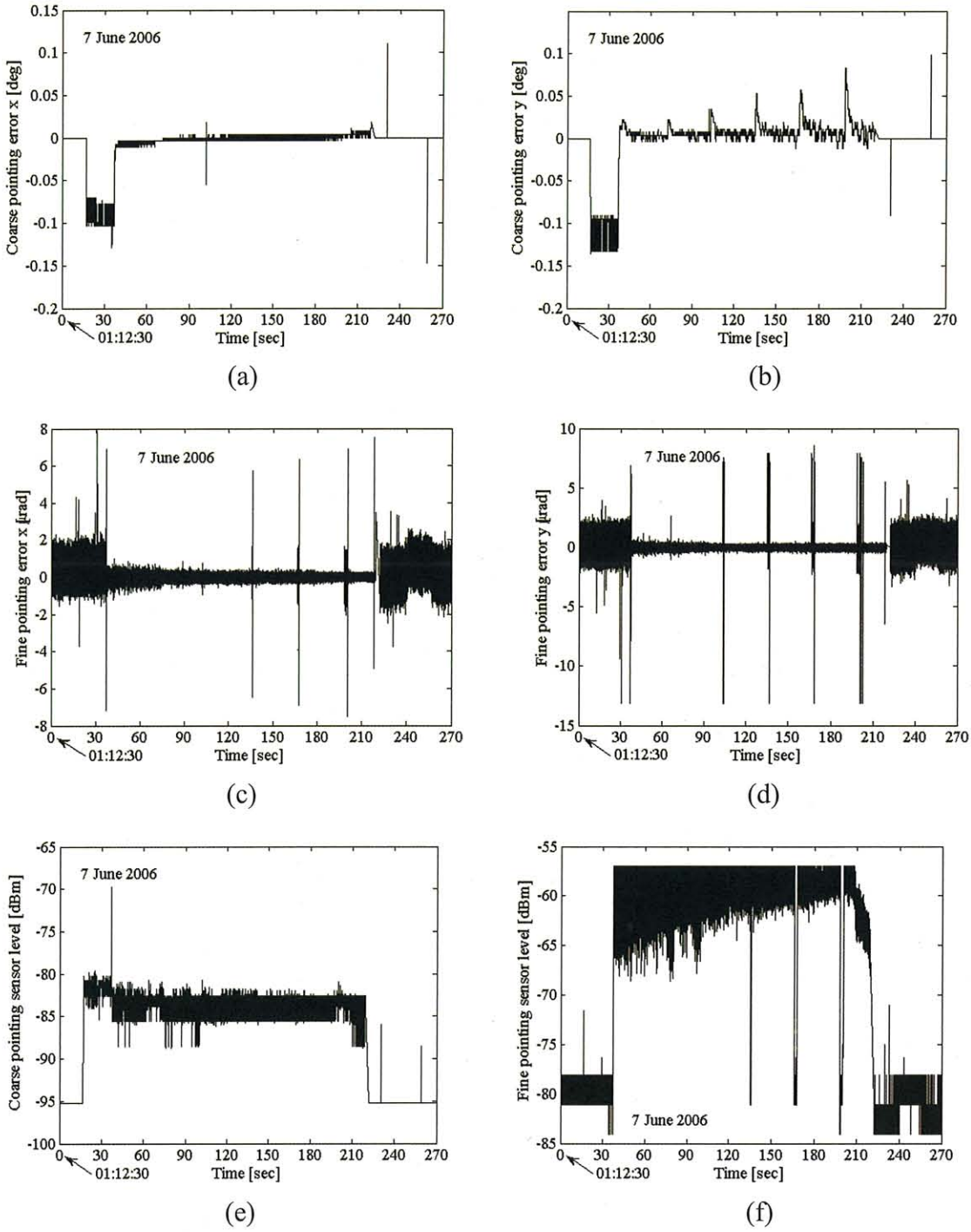

Figure 8.2.3-1 OICETS mission telemetries on 7th June, 2006. (a) Coarse pointing error X, (b) Coarse pointing error Y, (c) Fine pointing error X, (d) Fine pointing error Y, (e) Coarse pointing sensor level and (f) Fine pointing sensor level.

8.3 Second trial on 9th June, 2006

Due to some wrong procedures, JAXA failed to send the CPF file to DLR. DLR carried out the second trial with the orbit information of the two line elements.

8.3.1 Configuration and predictions

KIODO Experiment Configuration Sheet

Revision: 1
Date: 2006/6/8

Experiment date:	9th June 2006
Planning Time (UT)	00:02:29 - 00:05:38
Test Objective	Downlink

S/C: OICETS

No.	Parameter	Setting	Note
1	LD 1 or 2	LD1	nominal case: 1
2	LD modulation mode (PN or CW)	PN	
3	LD output power (100mW or 80mW)	100mW	

DLR Ground station

No.	Parameter	Setting	Note
1	Wavelength	809 nm	
2	Total Beacon Power	0.15 W	at 90° elevation (It was 0.3 W in Trial #1)
3	Divergence angle	5 mrad	FWHM
4	Power percentage for beacons	50, 50	beacons at 809 nm
5	Mode of beacon power	adjustable	
6	Power percentage for instruments	8, 4, 4, 42, 42	Rx, Tracking, Profiler, DIMM, Powermeter
7	Exposure of DIMM and Profiler	150 μs, 100 μs	for DIMM and profiler, respectively

Figure 8.3.1-1 Configuration sheet.

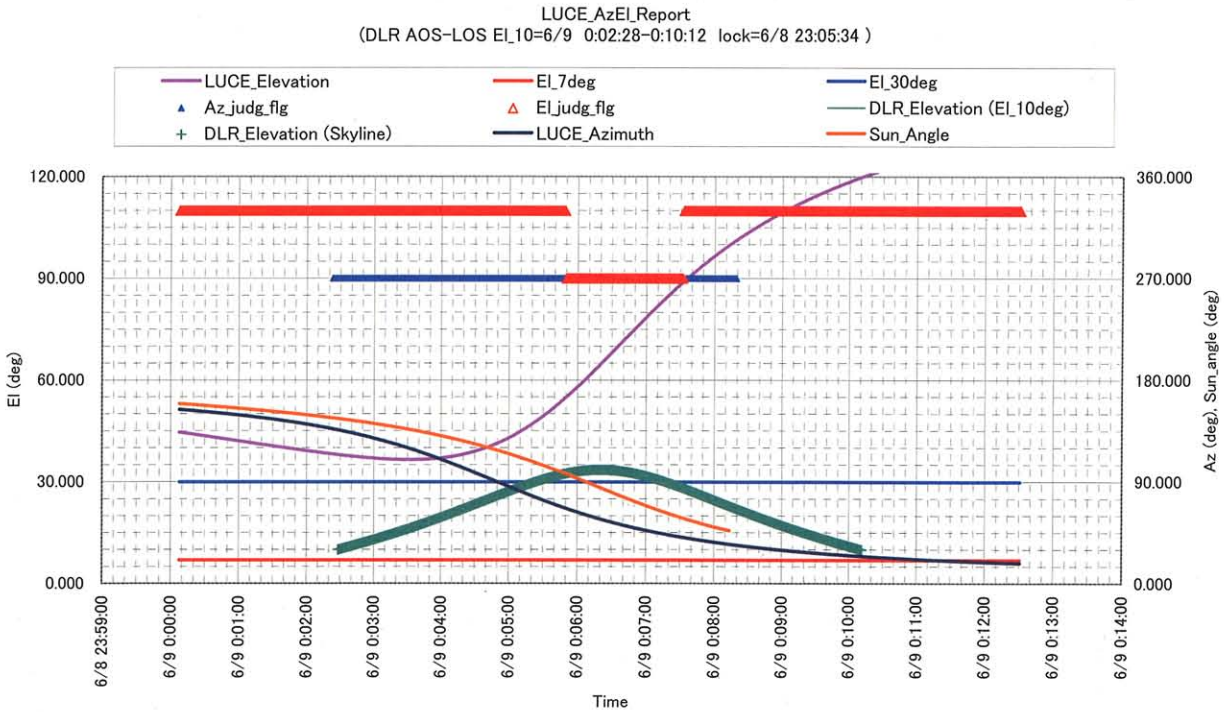

Figure 8.3.1-2 Predictions on angular movements of OGS and LUCE

8.3.2 OGS measurement

During Trial #2, no BER could be measured because wrong settings have been inadvertently used.

Weather at OGS-OP during experiment: 90% clear sky, 10°C

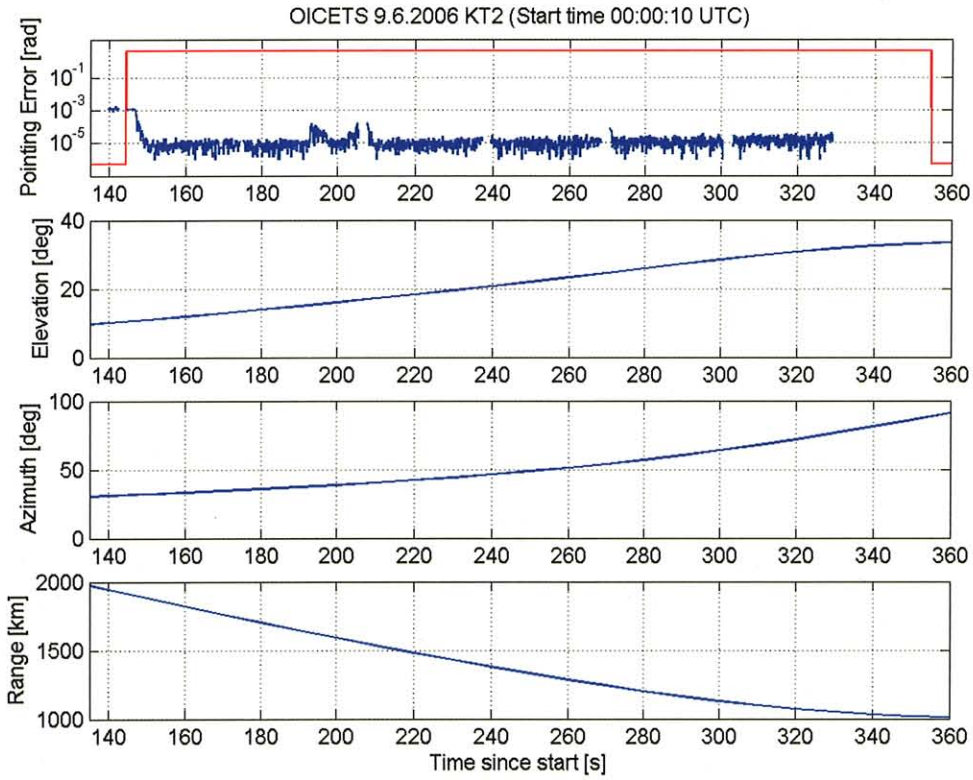

Figure 8.3.2-1 Pointing error of OGS-OP along with link parameters for Trial #2. The binary line in the pointing-error graph is high when the narrow-field-of-view camera is used and low when the large-field-of-view camera is used.

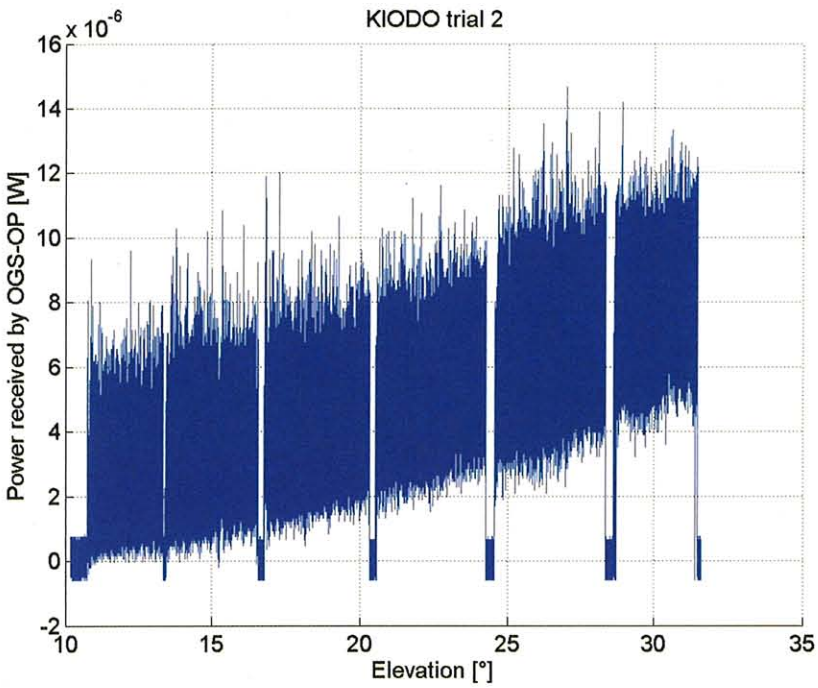

Figure 8.3.2-2 Optical Power impinging on 40-cm telescope in Trial #2 (PIN diode in optical system).

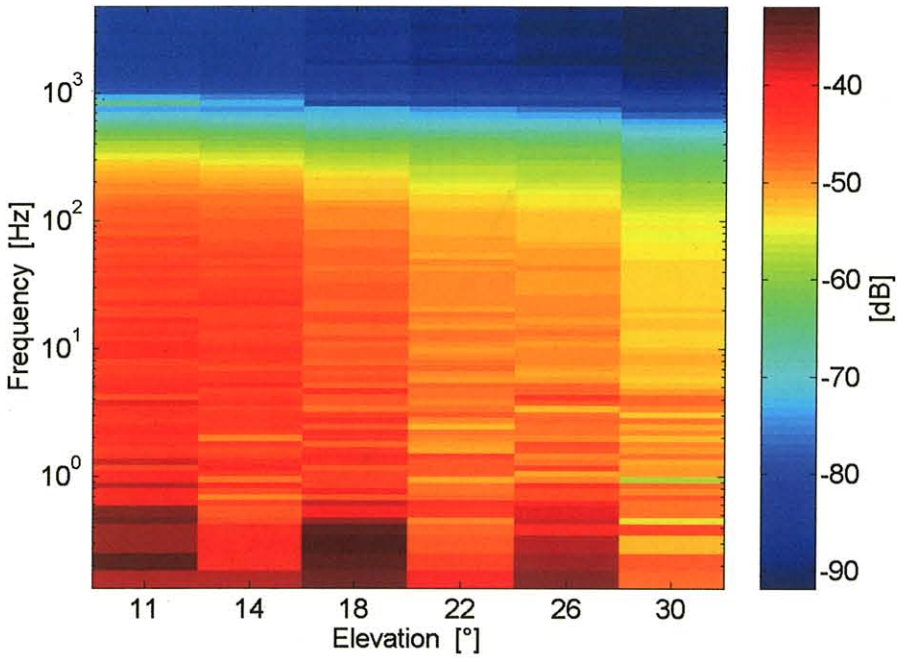

Figure 8.3.2-3 KT2: Spectrogram of the optical power received by the 40-cm telescope

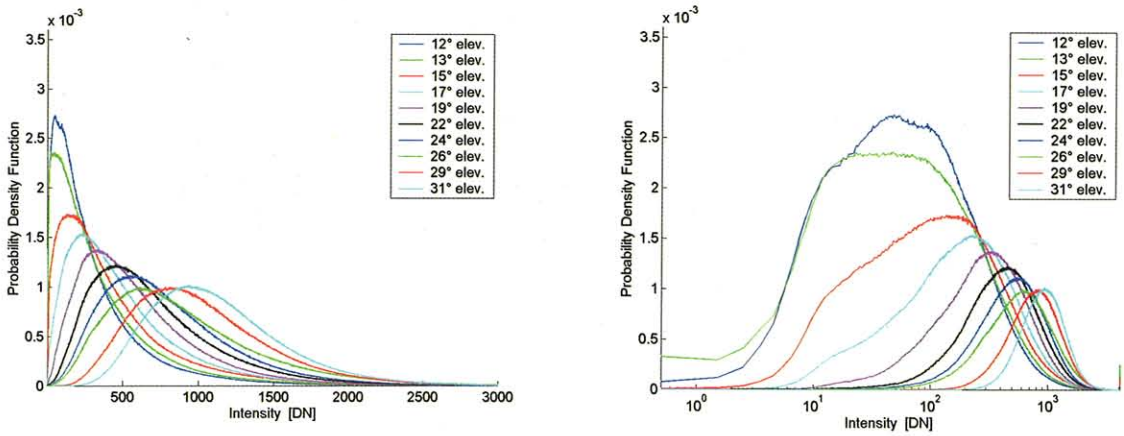

Linear scale Logarithmic scale

Figure 8.3.2-4 PDF of the intensity for Trial #2. The intensity corresponds to the pixel value of the profiler camera (DN = Digital Number)

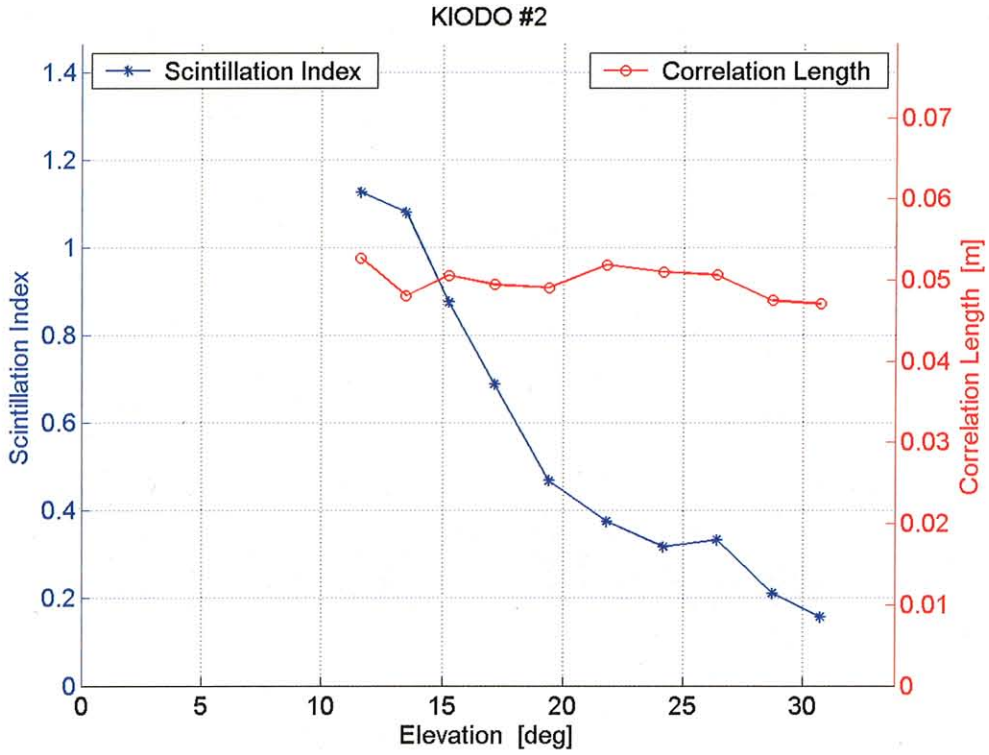

Figure 8.3.2-5 Intensity statistics for Trial #2.

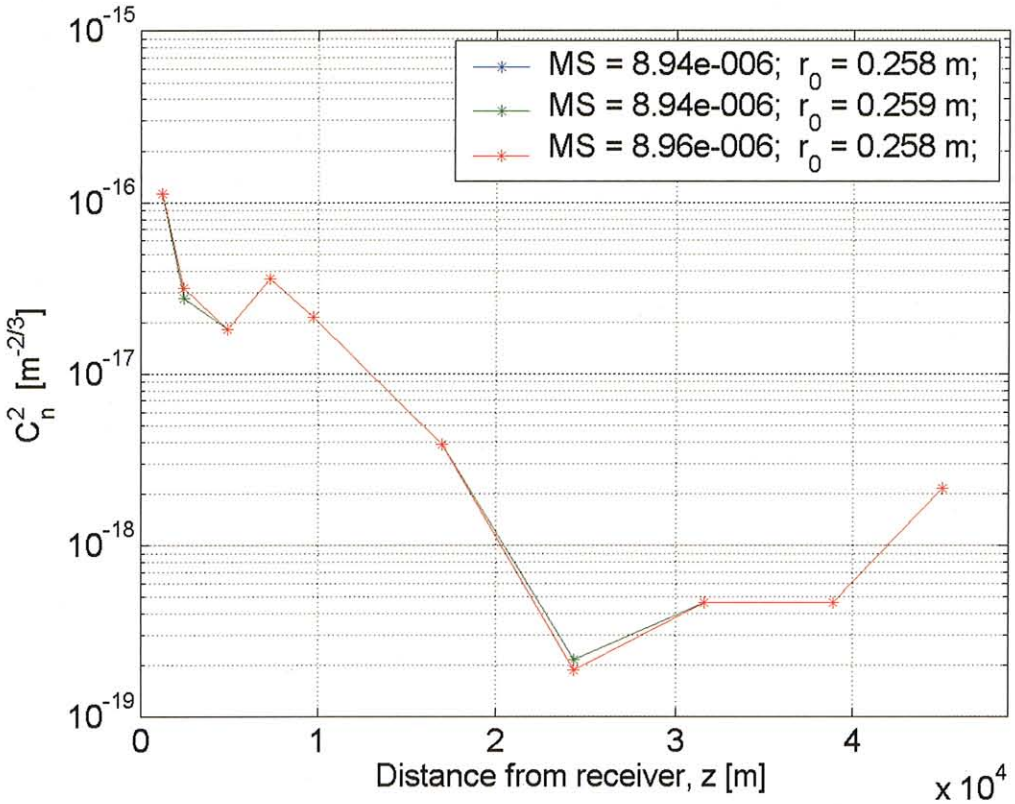

Figure 8.3.2-6 C_n^2 Profile derived from scintillation statistics at 31° elevation of Trial #2.

8.3.3 OICETS measurement

The coarse pointing sensor detected the beacon light from the OGS around 00:01:54, and the acquisition time was 157 msec.

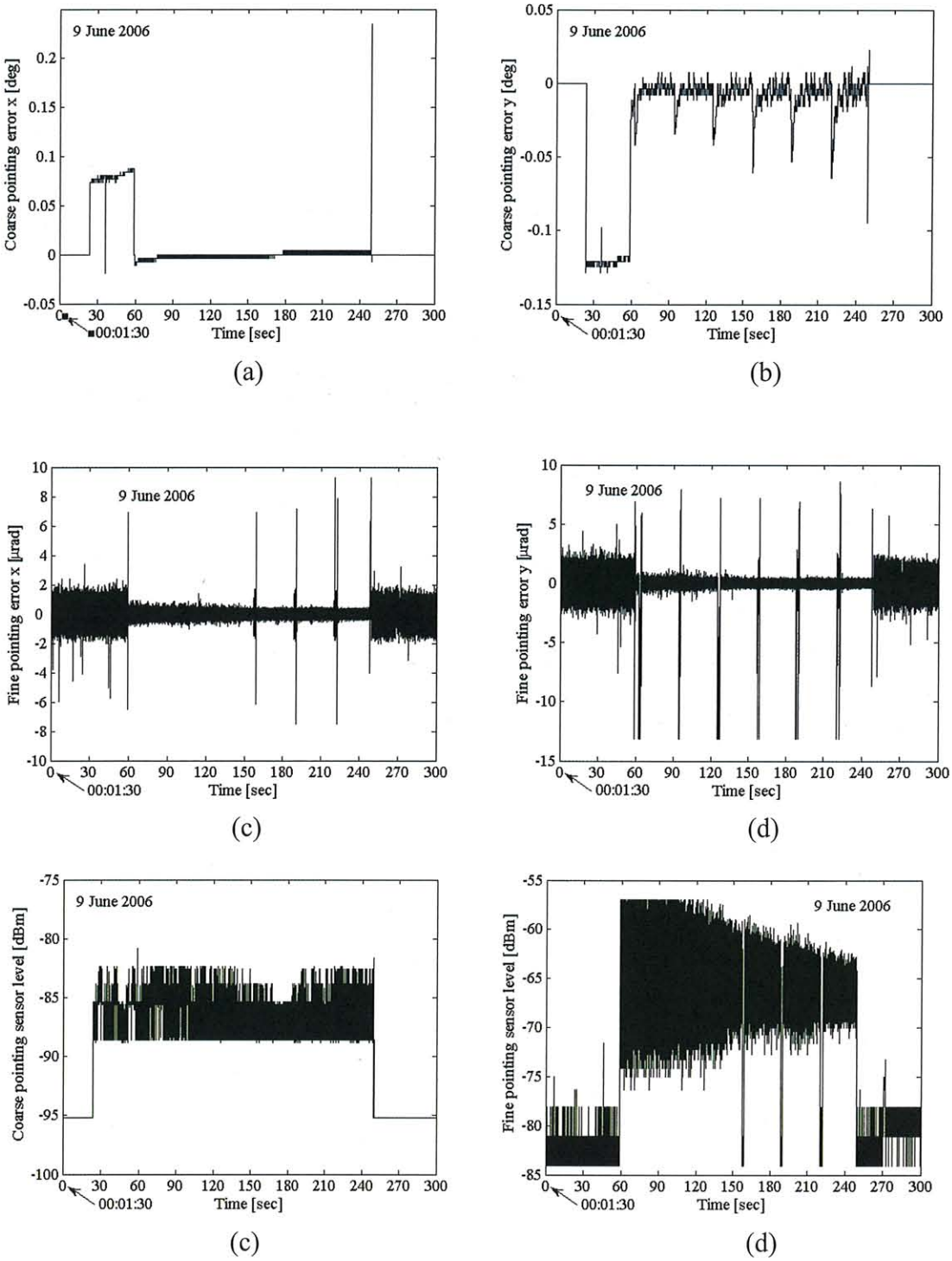

Figure 8.3.3-1 OICETS mission telemetries on 9th June, 2006. (a) Coarse pointing error X, (b) Coarse pointing error Y, (c) Fine pointing error X, (d) Fine pointing error Y, (e) Coarse pointing sensor level and (f) Fine pointing sensor level.

8.4 Third trial on 14th June, 2006

8.4.1 Configuration and predictions

KIODO Experiment Configuration Sheet

Revision: 1
Date: 2006/6/13

Experiment date:	14th June 2006
Planning Time (UT)	01:04:46−01:07:57
Test Objective	Downlink

S/C: OICETS

No.	Parameter	Setting	Note
1	LD 1 or 2	LD1	nominal case: 1
2	LD modulation mode (PN or CW)	PN	
3	LD output power (100mW or 80mW)	100mW	

DLR Ground station

No.	Parameter	Setting	Note
1	Wavelength	809 nm	
2	Total Beacon Power	0.15 W, 5 W	at 90°and 10° elevation, respectively
3	Divergence angle	5 mrad	FWHM
4	Power percentage for beacons	50, 50	beacons at 809 nm
5	Mode of beacon power	adjustable	
6	Power percentage for instruments	8, 4, 4, 42, 42	Rx, Powermeter, Tracking, Profiler, DIMM
7	Exposure of DIMM and Profiler	150 μs, 100 μs	for DIMM and profiler, respectively

Figure 8.4.1-1 Configuration sheet.

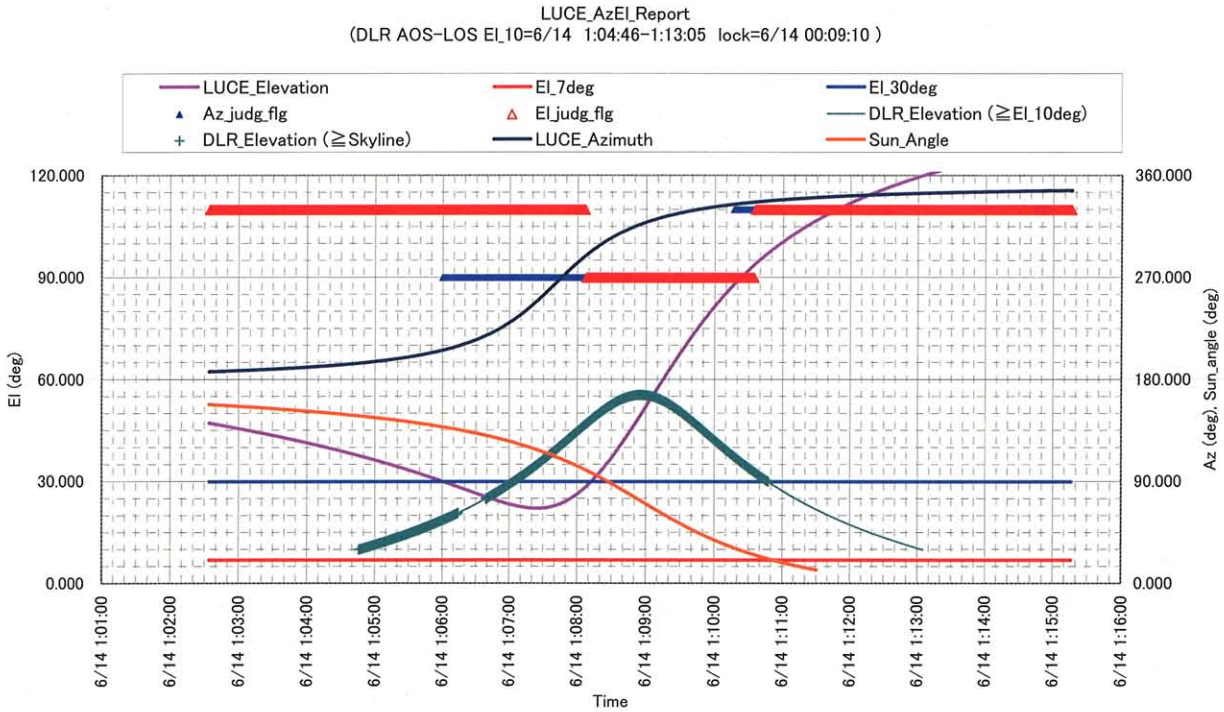

Figure 8.4.1-2 Predictions on angular movements of OGS and LUCE

8.4.2 OGS measurement

Weather at OGS-OP during experiment: clear sky, 10°C

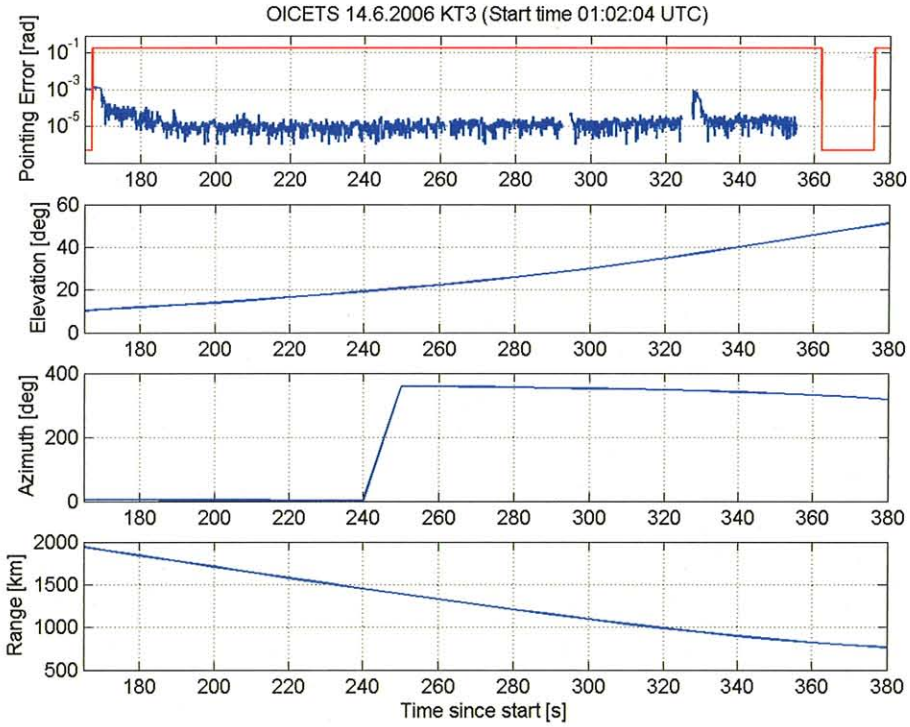

Figure 8.4.2-1 Pointing error of OGS-OP along with link parameters for Trial #3. The binary line in the pointing-error graph is high when the narrow-field-of-view camera is used and low when the large-field-of-view camera is used.

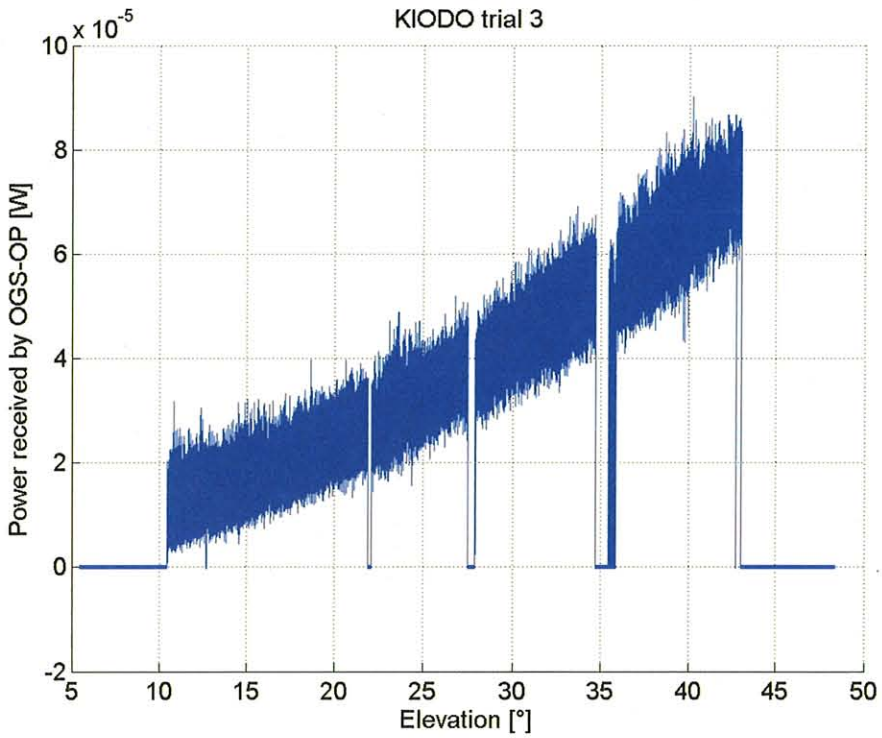

Figure 8.4.2-2 Optical Power impinging on 40-cm telescope in Trial #3 (PIN diode in optical system).

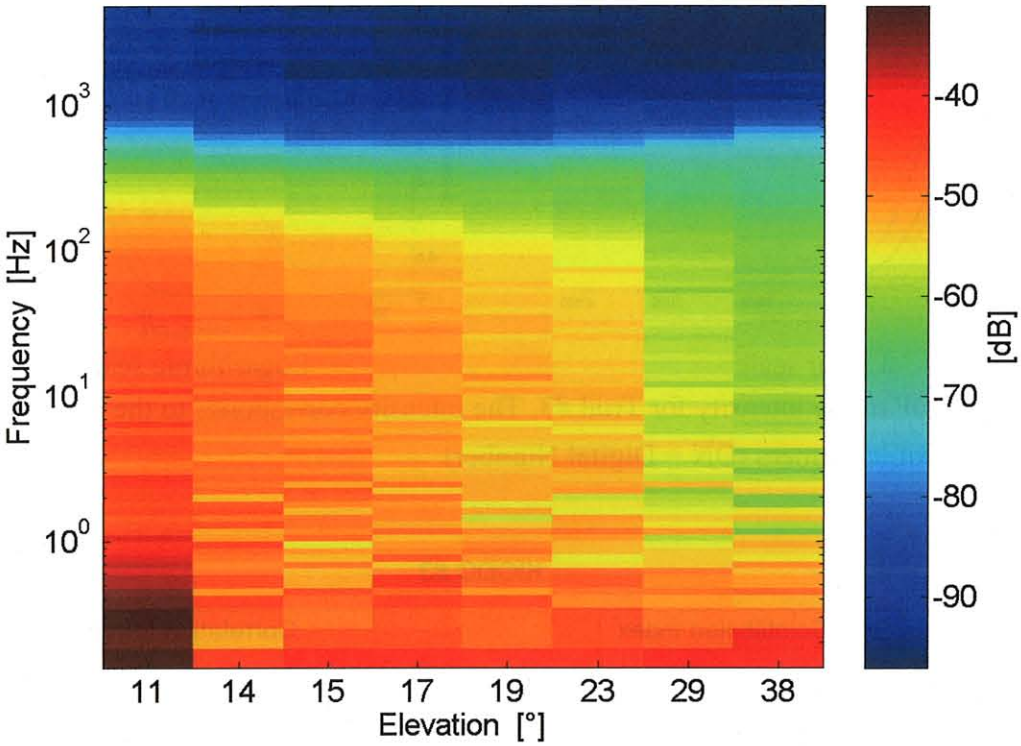

Figure 8.4.2-3 KT3: Spectrogram of the optical power received by the 40-cm telescope

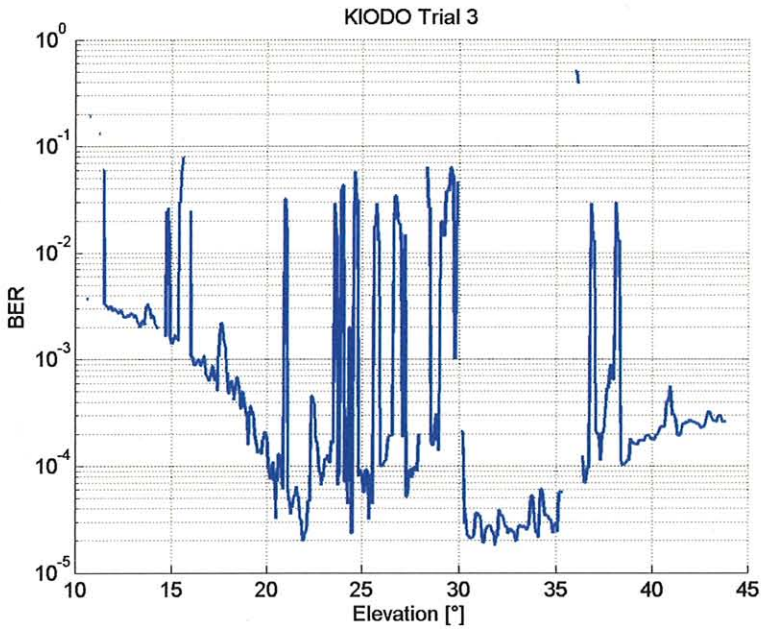

Figure 8.4.2-4 Bit error rate of Trial #3.

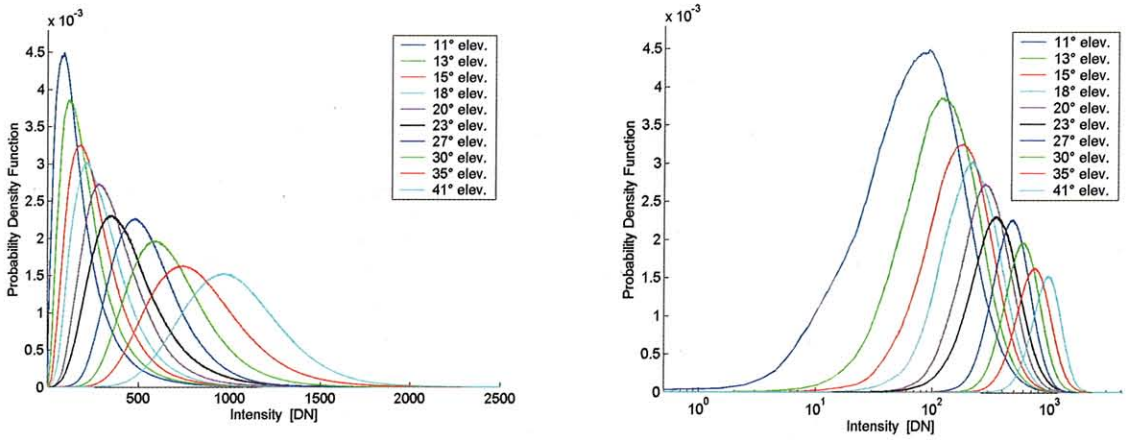

Linear scale Logarithmic scale

Figure 8.4.2-5 PDF of the intensity for Trial #3. The intensity corresponds to the pixel value of the profiler camera (DN = Digital Number)

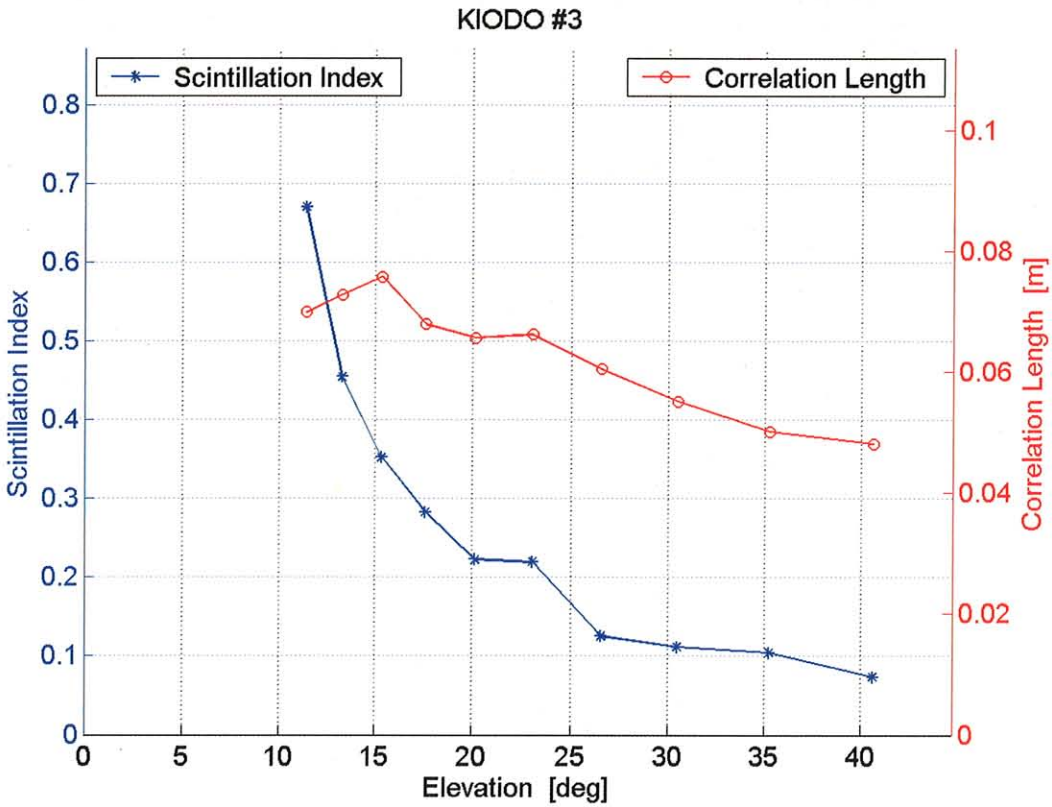

Figure 8.4.2-6 Intensity statistics of Trial #3.

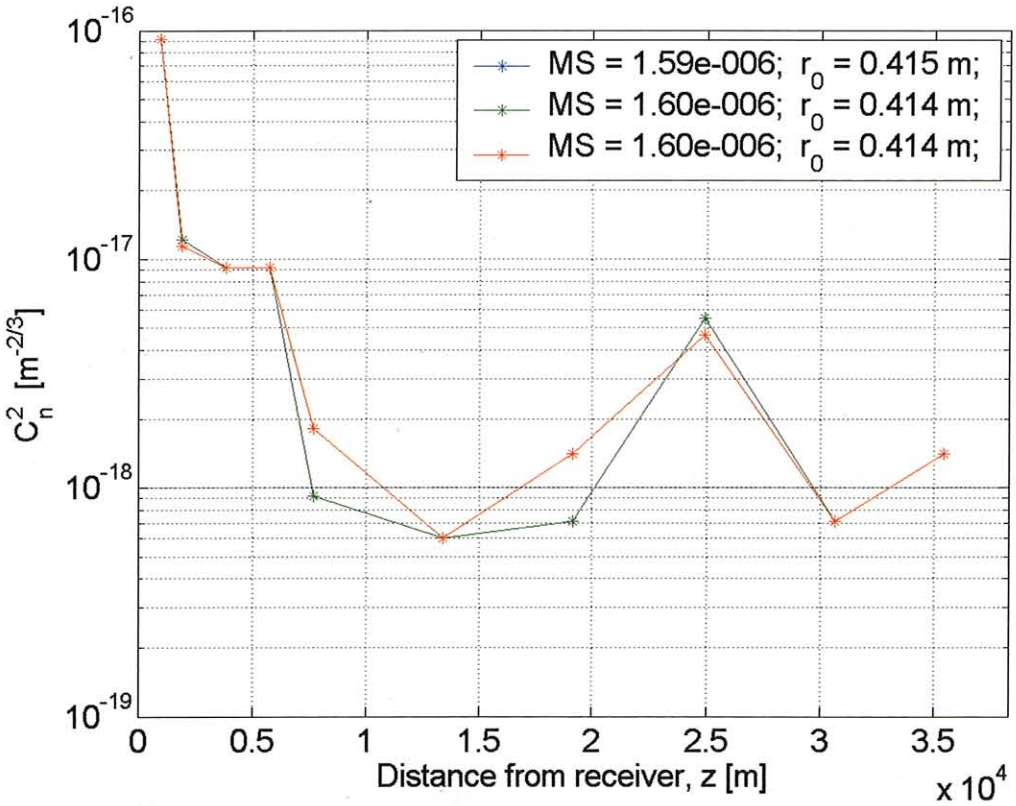

Figure 8.4.2-7 C_n^2 Profile derived from scintillation statistics at 41° elevation of Trial #3.

8.4.3 OICETS measurement

The coarse pointing sensor detected the beacon light from the OGS around 01:04:26, and the acquisition time was 70 msec.

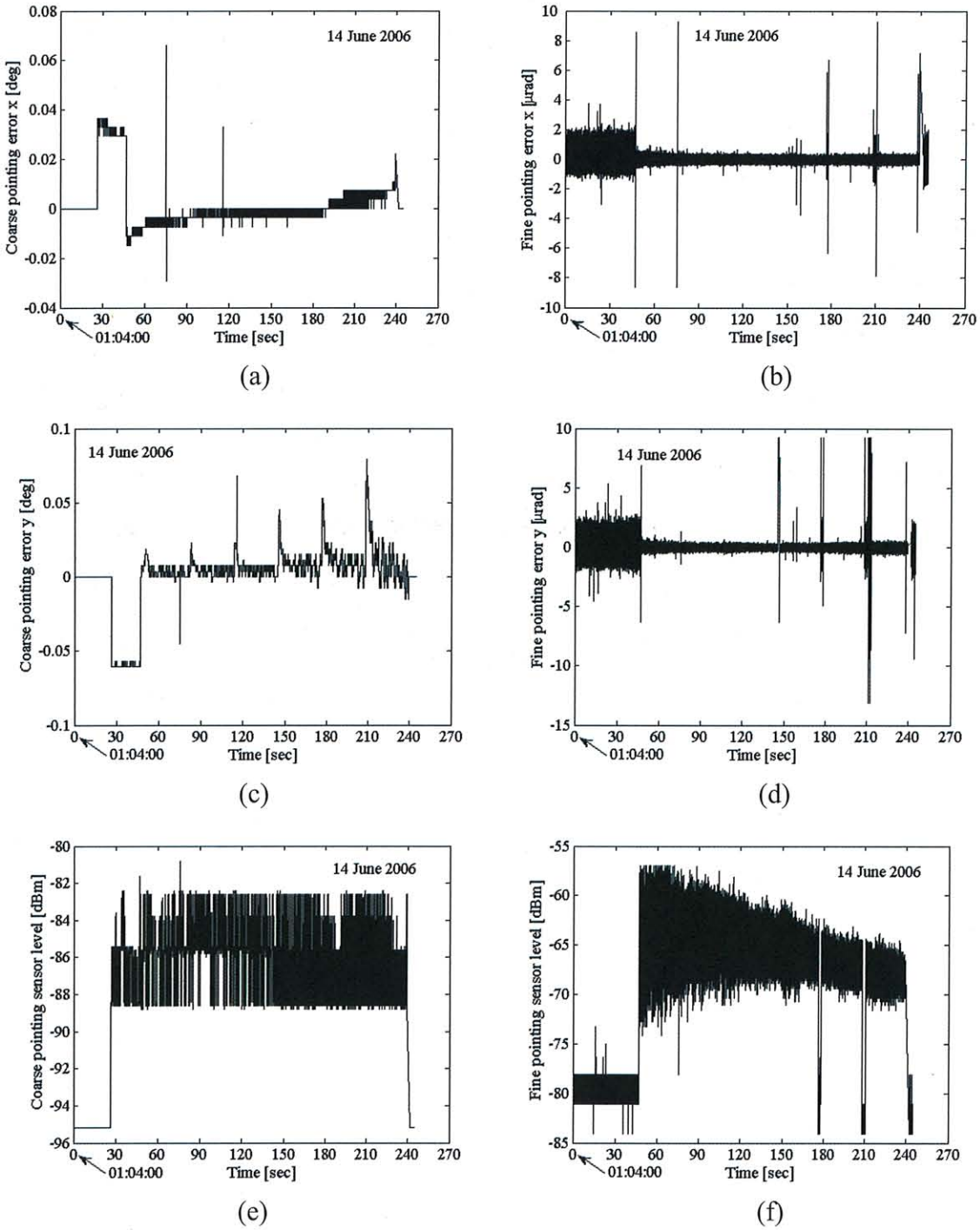

Figure 8.4.3-1 OICETS mission telemetries on 14th June, 2006. (a) Coarse pointing error X, (b) Coarse pointing error Y, (c) Fine pointing error X, (d) Fine pointing error Y, (e) Coarse pointing sensor level and (f) Fine pointing sensor level.

8.5 Forth trial on 15th June, 2006

8.5.1 Configuration and predictions

KIODO Experiment Configuration Sheet

Revision: 1
Date: 2006/6/15

Experiment date:	15th June 2006
Planning Time (UT)	23:51:52−23:57:19
Test Objective	Downlink. DLR beacon exposure at 0-elevation angle

S/C: OICETS

No.	Parameter	Setting	Note
1	LD 1 or 2	LD1	nominal case: 1
2	LD modulation mode (PN or CW)	PN	
3	LD output power (100mW or 80mW)	100mW	

DLR Ground station

No.	Parameter	Setting	Note
1	Wavelength	809 nm	
2	Total Beacon Power	0.15 W, 5 W	at 90°and 10° elevation, respectively
3	Divergence angle	5 mrad	FWHM
4	Power percentage for beacons	50, 50	beacons at 809 nm
5	Mode of beacon power	adjustable	
6	Power percentage for instruments	(less than 8), 4, 4, 42, 42	Rx, Powermeter, Tracking, Profiler, DIMM
7	Exposure of DIMM and Profiler	150 μs, 100 μs	for DIMM and profiler, respectively

Figure 8.5.1-1 Configuration sheet.

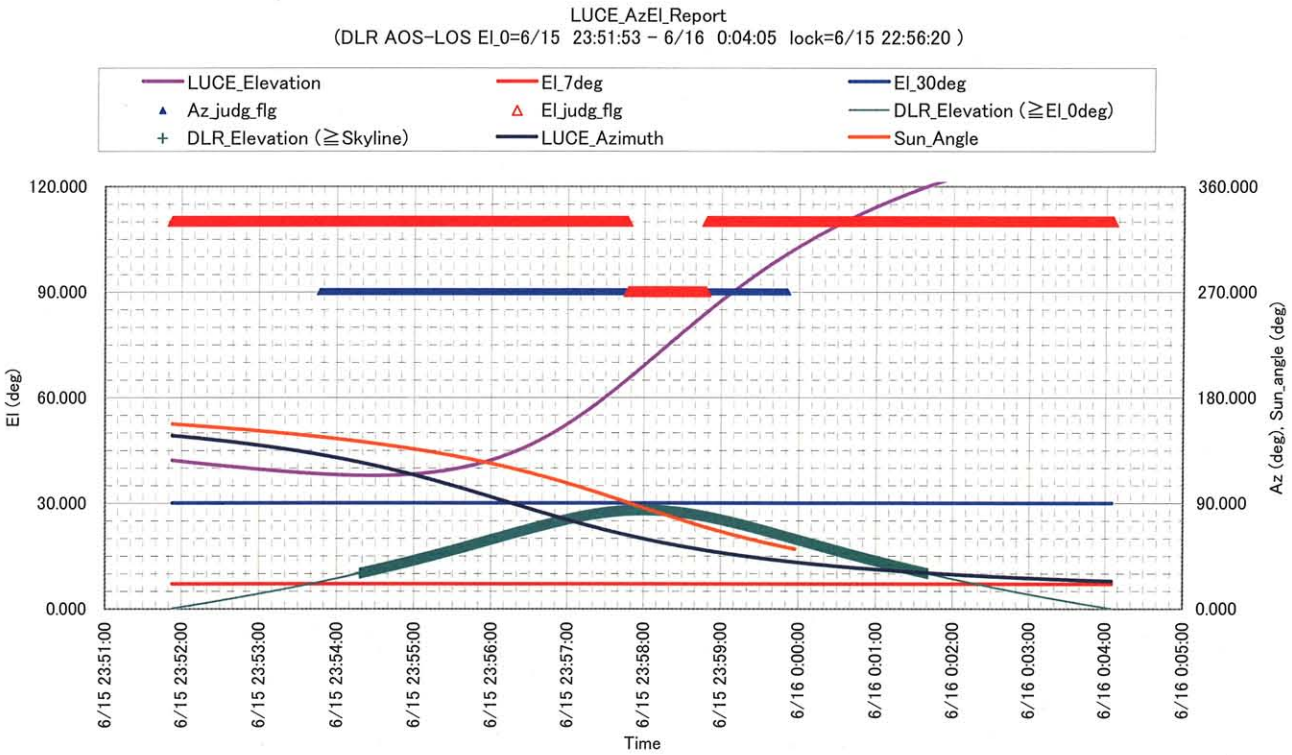

Figure 8.5.1-2 Predictions on angular movements of OGS and LUCE

8.5.2 OGS measurement

Weather at OGS-OP: stars visible at 23:00, more clouds at trial, supposedly one cloud in link path.

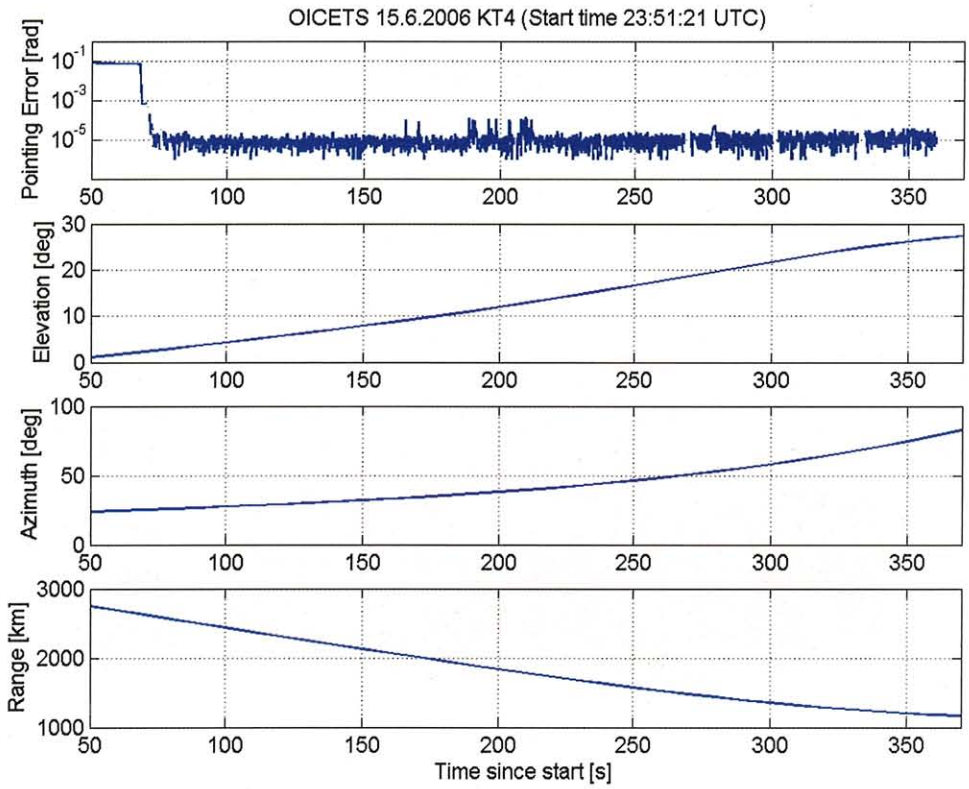

Figure 8.5.2-1 Pointing error of OGS-OP along with link parameters for Trial #4.

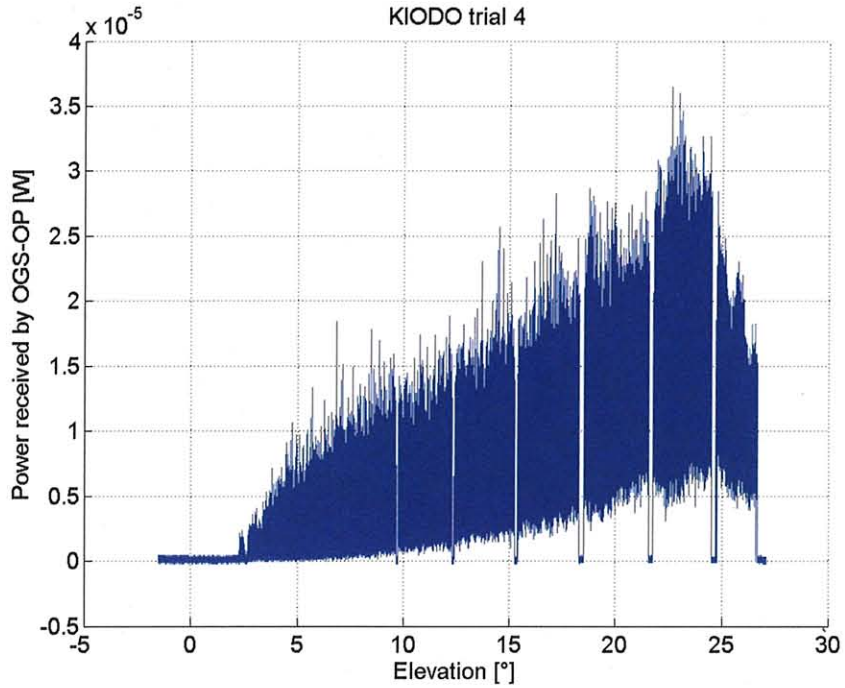

Figure 8.5.2-2 Optical Power impinging on 40-cm telescope in Trial #4 (PIN diode in optical system).

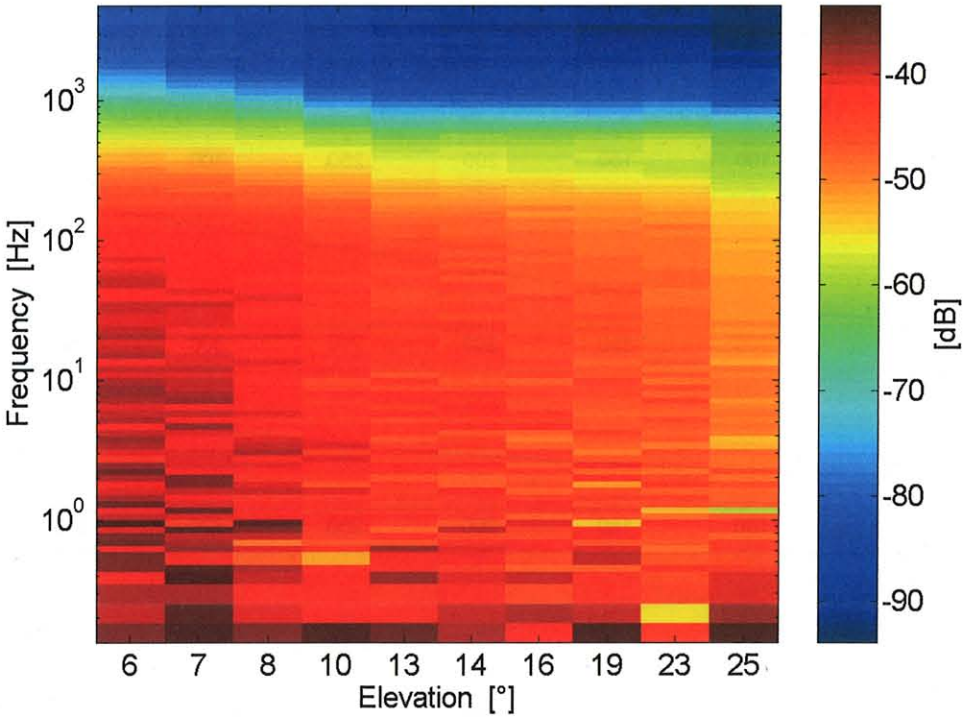

Figure 8.5.2-3 KT4: Spectrogram of the optical power received by the 40-cm telescope

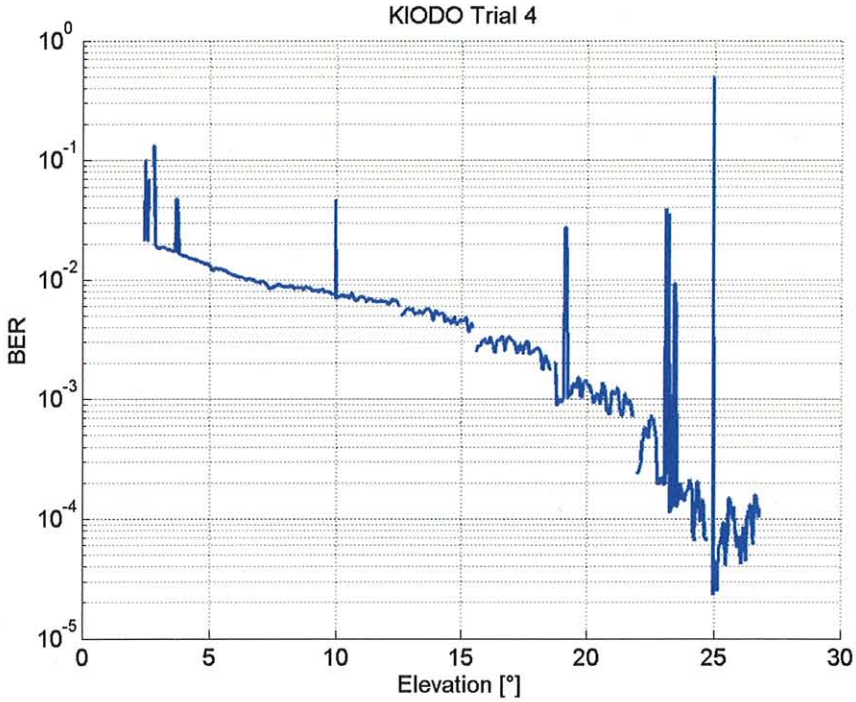

Figure 8.5.2-4 Bit error rate of Trial #4.

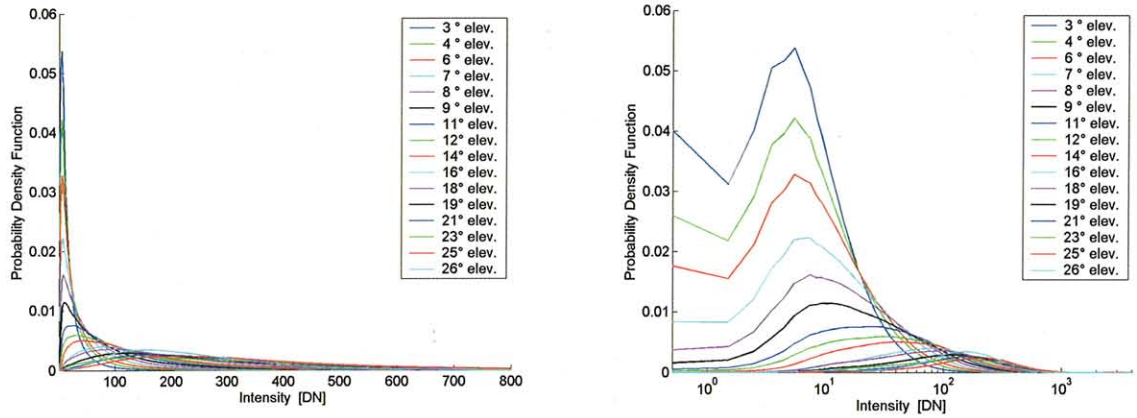

Linear scale Logarithmic scale

Figure 8.5.2-5 PDF of the intensity for Trial #4. The intensity corresponds to the pixel value of the profiler camera (DN = Digital Number)

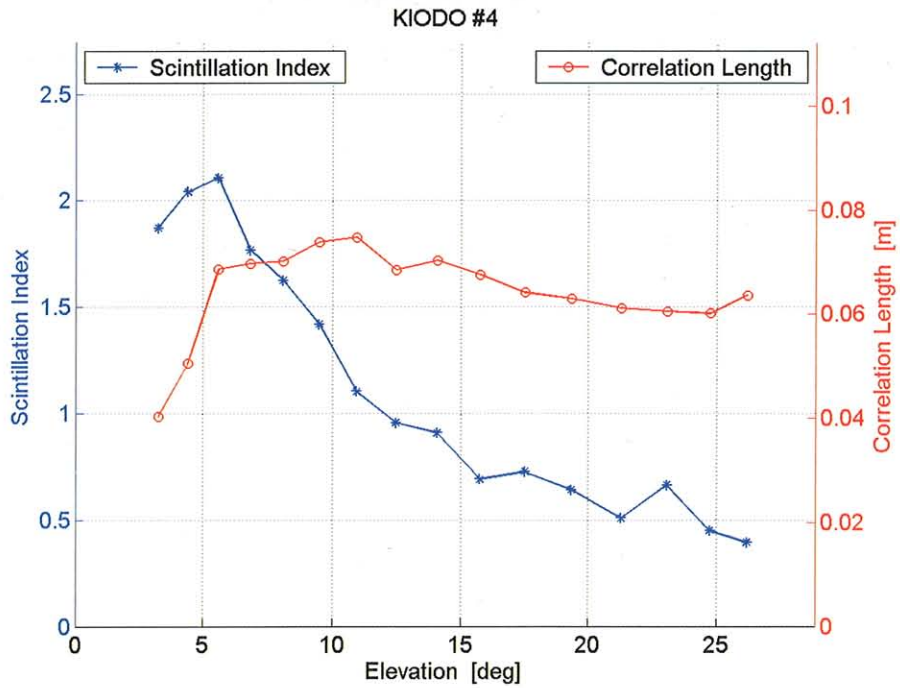

Figure 8.5.2-6 Intensity statistics of Trial #4.

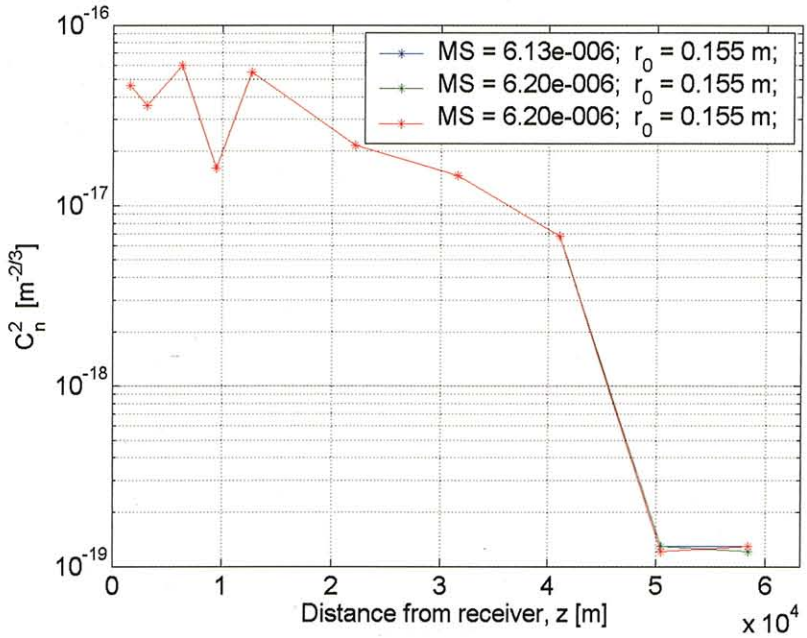

Figure 8.5.2-7 C_n^2 Profile derived from scintillation statistics at 26° elevation of Trial #4.

8.5.3 OICETS measurement

The coarse pointing sensor detected the beacon light from the OGS around 23:52:14, and the acquisition time was 310 msec.

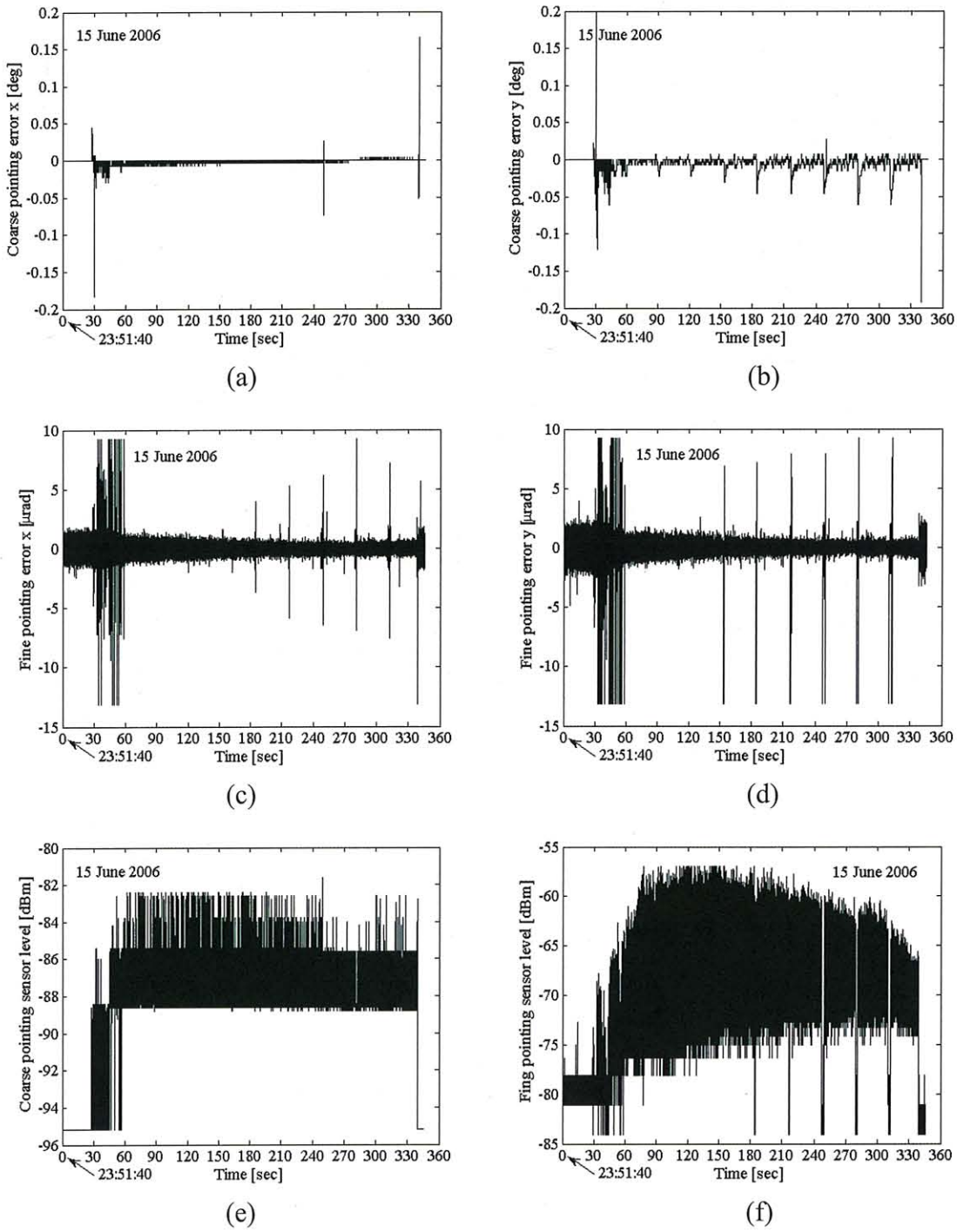

Figure 8.5.3-1 OICETS mission telemetries on 15th June, 2006. (a) Coarse pointing error X, (b) Coarse pointing error Y, (c) Fine pointing error X, (d) Fine pointing error Y, (e) Coarse pointing sensor level and (f) Fine pointing sensor level.

8.6 Fifth trial on 21st June, 2006

8.6.1 Configuration and predictions

KIODO Experiment Configuration Sheet

Revision: 1
Date: 20 June 2006

Experiment date:	21 June 2006
Planning Time (UT)	00:54:12−00:59:42
Test Objective	Downlink. DLR beacon exposure at 0-elevation angle

S/C: OICETS

No.	Parameter	Setting	Note
1	LD 1 or 2	LD1	nominal case: 1
2	LD modulation mode (PN or CW)	PN	
3	LD output power (100mW or 80mW)	100mW	

DLR Ground station

No.	Parameter	Setting	Note
1	Wavelength	809 nm	
2	Total Beacon Power	0.15 W, 5 W	at 90°and 10° elevation, respectively
3	Divergence angle	8 mrad	FWHM
4	Power percentage for beacons	50, 50	beacons at 809 nm
5	Mode of beacon power	adjustable	
6	Power percentage for instruments	8, 4, 4, 42, 42	Rx, Powermeter, Tracking, Profiler, DIMM
7	Exposure of DIMM and Profiler	150 μs, 100 μs	for DIMM and profiler, respectively

The link was not established due to the weather conditions.

8.7 Sixth trial on 23rd June, 2006

8.7.1 Configuration and predictions

KIODO Experiment Configuration Sheet

Revision: 1

Date: 22 June 2006

Experiment date:	23 June 2006
Planning Time (UT)	01:19:17−01:24:30
Test Objective	Downlink. DLR beacon exposure at 0-elevation angle

S/C: OICETS

No.	Parameter	Setting	Note
1	LD 1 or 2	LD1	nominal case: 1
2	LD modulation mode (PN or CW)	PN	
3	LD output power (100mW or 80mW)	100mW	

DLR Ground station

No.	Parameter	Setting	Note
1	Wavelength	809 nm	
2	Total Beacon Power	0.15 W, 5 W	at 90°and 10° elevation, respectively
3	Divergence angle	5 mrad	FWHM
4	Power percentage for beacons	50, 50	beacons at 809 nm
5	Mode of beacon power	adjustable	
6	Power percentage for instruments	8, 4, 4, 42, 42	Rx, Powermeter, Tracking, Profiler, DIMM
7	Exposure of DIMM and Profiler	150 μs, 100 μs	for DIMM and profiler, respectively

The link was not established due to the weather conditions.

8.8 Seventh trial on 28th June, 2006

8.8.1 Configuration and predictions

KIODO Experiment Configuration Sheet

Revision: 1
Date: 27 June 2006

Experiment date:	28 June 2006
Planning Time (UT)	01:19:17−01:24:30
Test Objective	Downlink. DLR beacon exposure at 0-elevation angle

S/C: OICETS

No.	Parameter	Setting	Note
1	LD 1 or 2	LD1	nominal case: 1
2	LD modulation mode (PN or CW)	PN	
3	LD output power (100mW or 80mW)	100mW	

DLR Ground station

No.	Parameter	Setting	Note
1	Wavelength	809 nm	
2	Total Beacon Power	0.15 W, 5 W	at 90°and 10° elevation, respectively
3	Divergence angle	5 mrad	FWHM
4	Power percentage for beacons	50, 50	beacons at 809 nm
5	Mode of beacon power	adjustable	
6	Power percentage for instruments	8, 4, 4, 42, 42	Rx, Powermeter, Tracking, Profiler, DIMM
7	Exposure of DIMM and Profiler	150 μs, 100 μs	for DIMM and profiler, respectively

Figure 8.8.1-1 Configuration sheet.

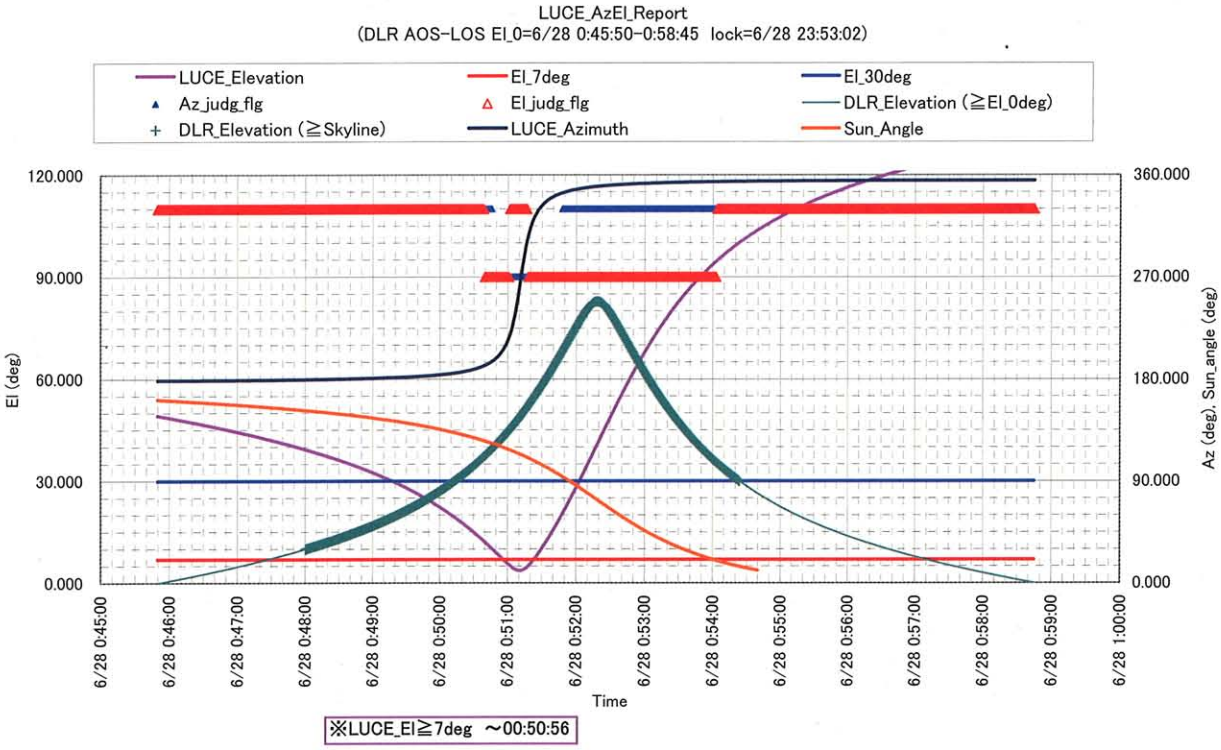

Figure 8.8.1-2 Predictions on angular movements of OGS and LUCE

8.8.2 OGS measurement

Weather at OGS-OP: Thunder clouds north one hour before experiment ; T = ~18°C

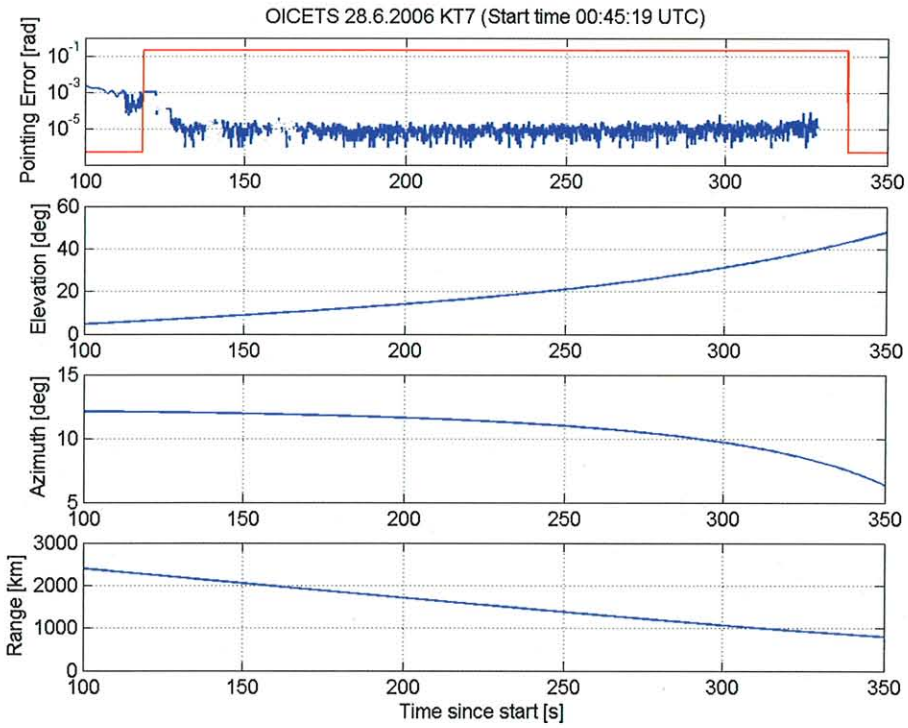

Figure 8.8.2-1 Pointing error of OGS-OP along with link parameters for Trial #7. The binary line in the pointing-error graph is high when the narrow-field-of-view camera is used and low when the large-field-of-view camera is used.

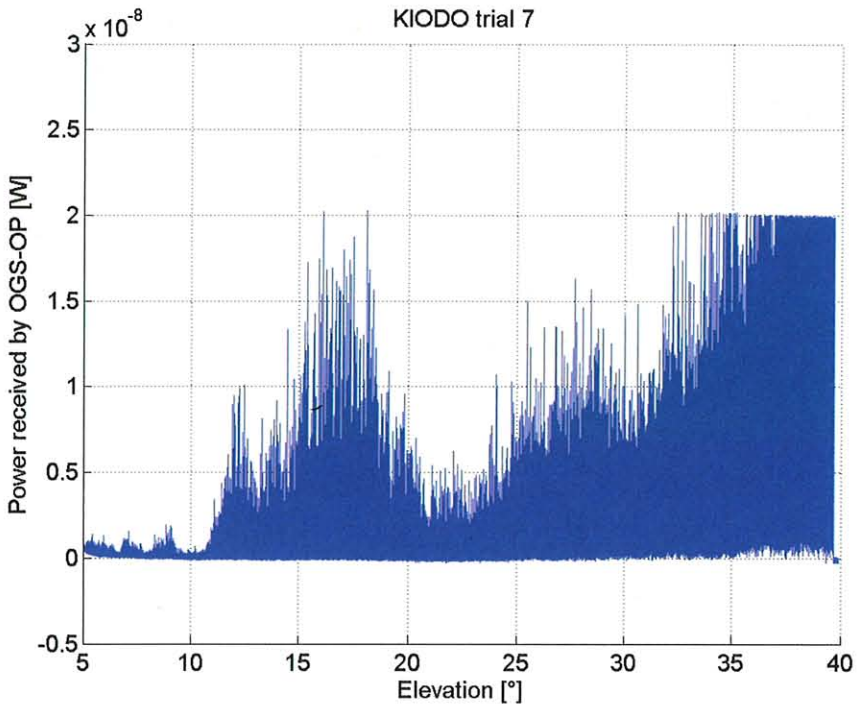

Figure 8.8.2-2 Optical Power received over a 5-cm telescope

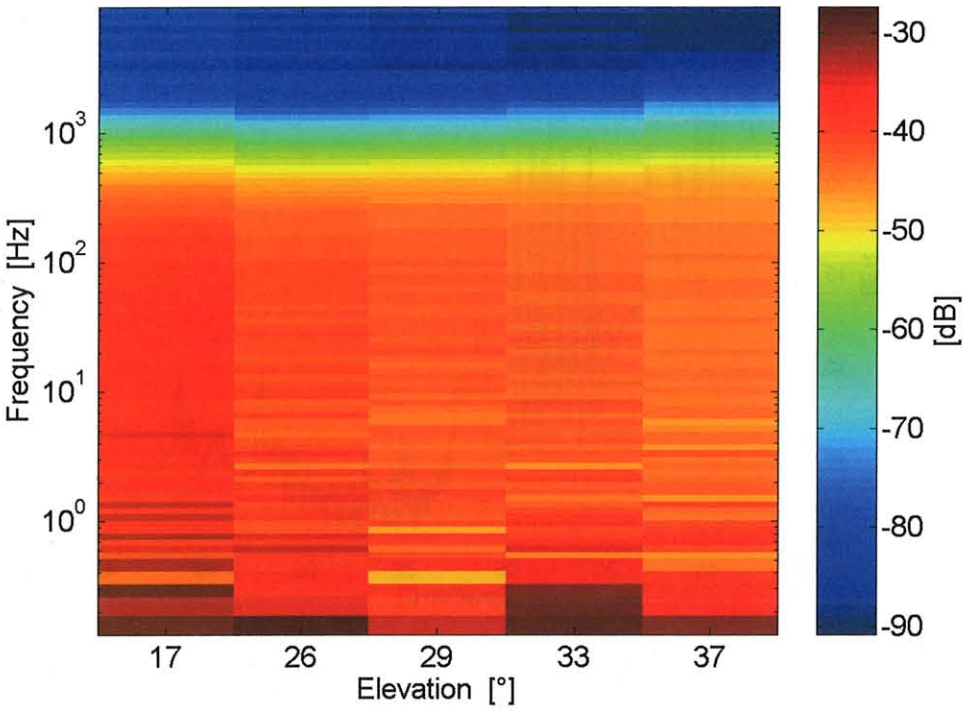

Figure 8.8.2-3 KT7: Spectrogram of the optical power received by the 5-cm telescope

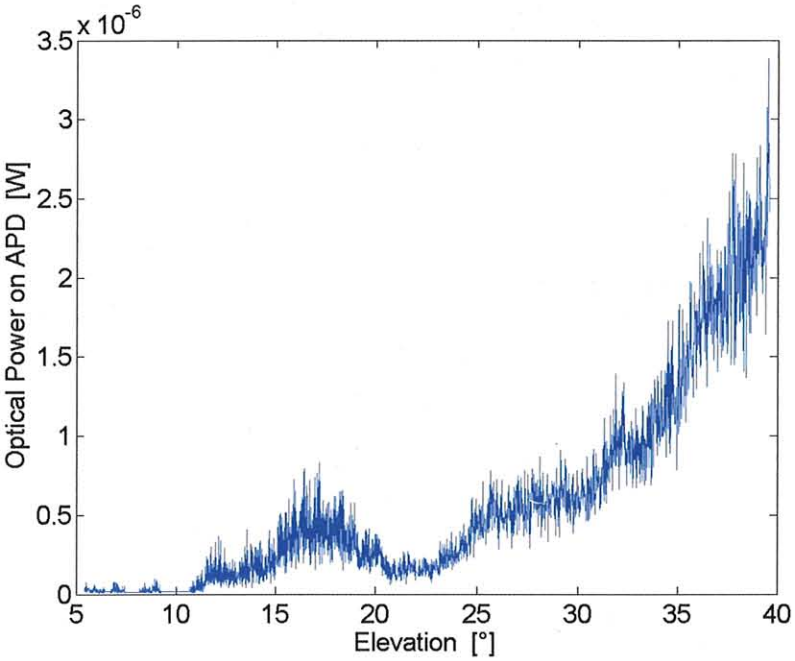

Figure 8.8.2-4 Optical Power received over a 40-cm telescope (calculated from the Profiler camera)

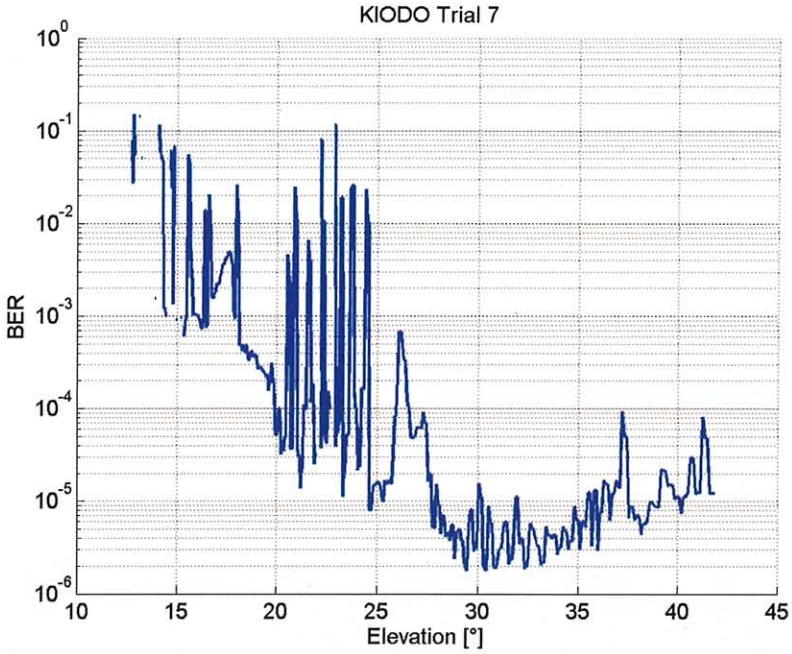

Figure 8.8.2-5 Bit error rate of Trial #7.

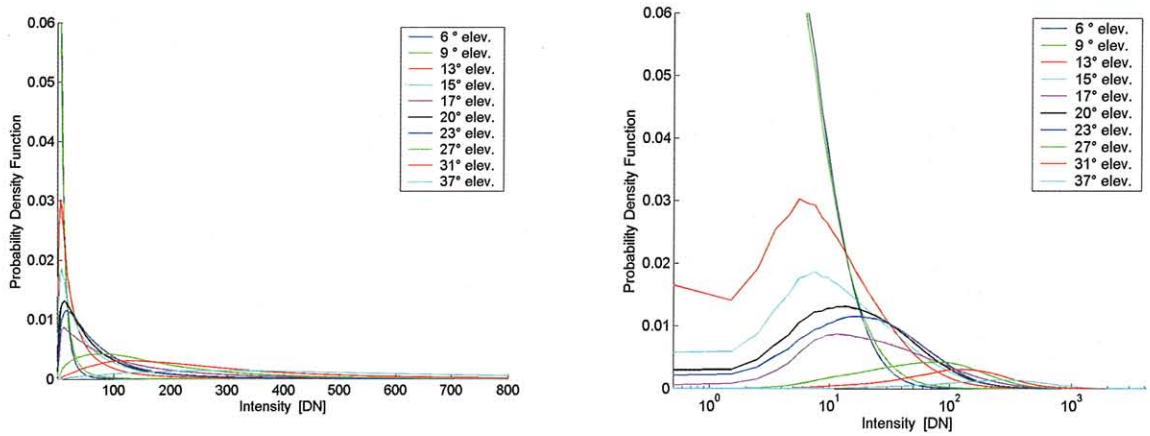

Linear scale Logarithmic scale

Figure 8.8.2-6 PDF of the intensity for Trial #7. The intensity corresponds to the pixel value of the profiler camera (DN = Digital Number).

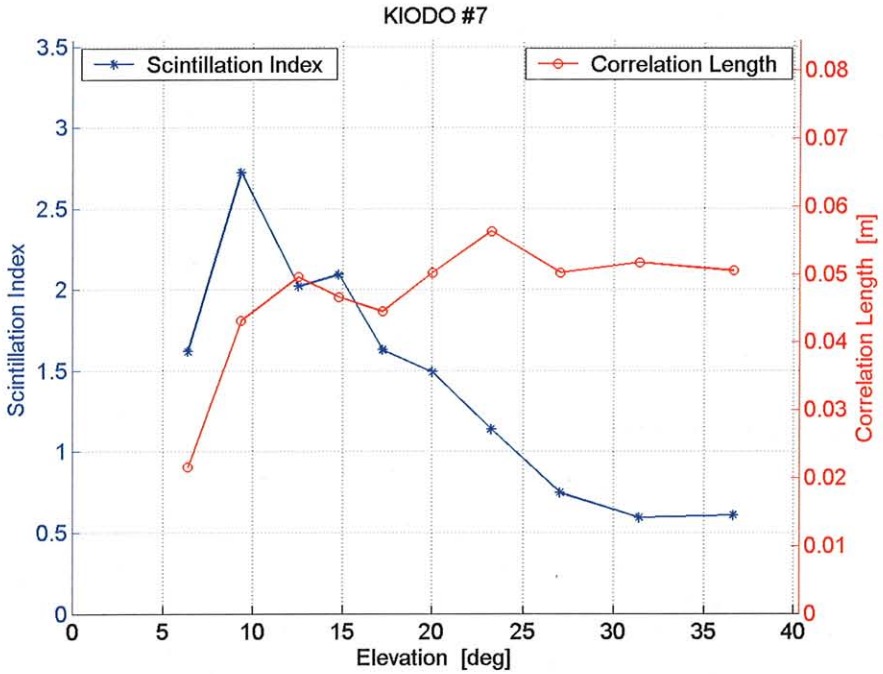

Figure 8.8.2-7 Intensity statistics of Trial #7.

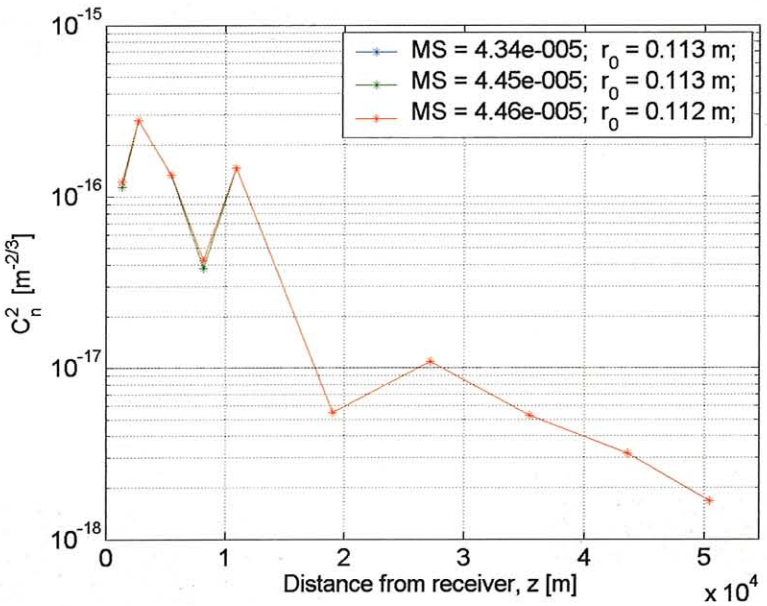

Figure 8.8.2-8 C_n^2 Profile derived from scintillation statistics at 37° elevation of Trial #7.

8.8.3 OICETS measurement

The coarse pointing sensor detected the beacon light from the OGS around 00:46:34, and the acquisition time was 120 msec.

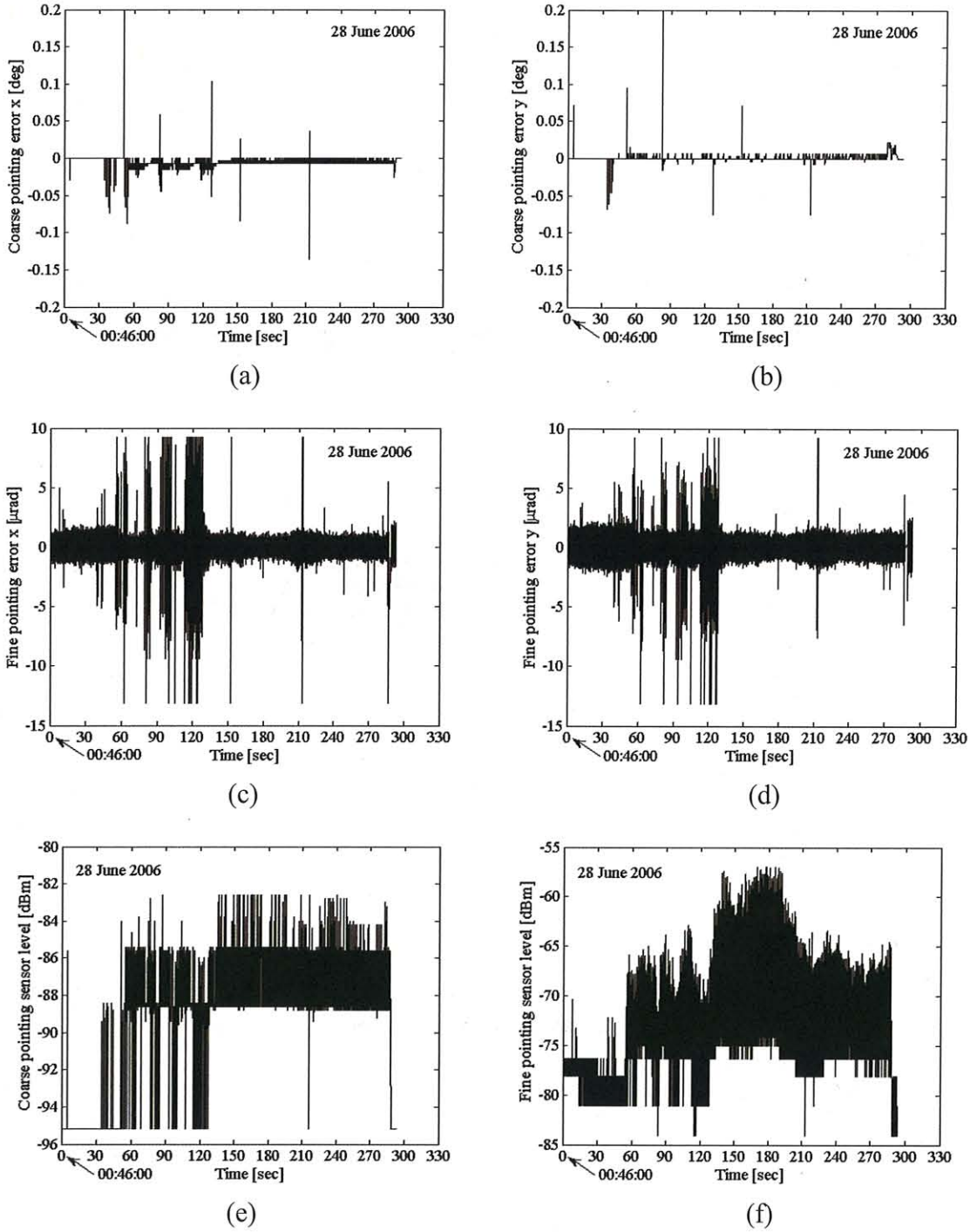

Figure 8.8.3-1 OICETS mission telemetries on 28th June, 2006. (a) Coarse pointing error X, (b) Coarse pointing error Y, (c) Fine pointing error X, (d) Fine pointing error Y, (e) Coarse pointing sensor level and (f) Fine pointing sensor level.

8.9 Eighth trial on 30th June, 2006

8.9.1 Configuration and predictions

KIODO Experiment Configuration Sheet

Revision: 1
Date: 29 June 2006

Experiment date:	30 June 2006
Planning Time (UT)	01:10:53−01:16:14
Test Objective	Downlink. DLR beacon exposure at 0-elevation angle

S/C: OICETS

No.	Parameter	Setting	Note
1	LD 1 or 2	LD1	nominal case: 1
2	LD modulation mode (PN or CW)	PN	
3	LD output power (100mW or 80mW)	100mW	

DLR Ground station

No.	Parameter	Setting	Note
1	Wavelength	809 nm	
2	Total Beacon Power	0.15 W, 5 W	at 90°and 10° elevation, respectively
3	Divergence angle	5 mrad	FWHM
4	Power percentage for beacons	50, 50	beacons at 809 nm
5	Mode of beacon power	adjustable	
6	Power percentage for instruments	8, 4, 4, 42, 42	Rx, Powermeter, Tracking, Profiler, DIMM
7	Exposure of DIMM and Profiler	150 μs, 100 μs	for DIMM and profiler, respectively

The link was not established due to the weather conditions.

9 Summarized results

9.1 OGS measurement

9.1.1 Scintillation and r_0 (Summary)

The downlink scintillation results are summarized in Figure 9.1.1-1, Figure 9.1.1-2 and Figure 9.1.1-3. The r_0 parameter estimated from the DIMM is summarized in Figure 9.1.1-4.

General agreement of measurements with scintillation theory (see e.g. Sections 12.5.2 and 12.5.3 of [AND05]). Because of low elevation angles, scintillation has saturated. The weak-fluctuation theory could not be used for the generation of the turbulence profiles.

Note that when scintillation is strong, the r0 parameter tends to be small (high scintillation indices during KT7 corresponds to a small r0 values)

A very large variation of the scintillation between two different nights (although clock time and elevation are unchanged).

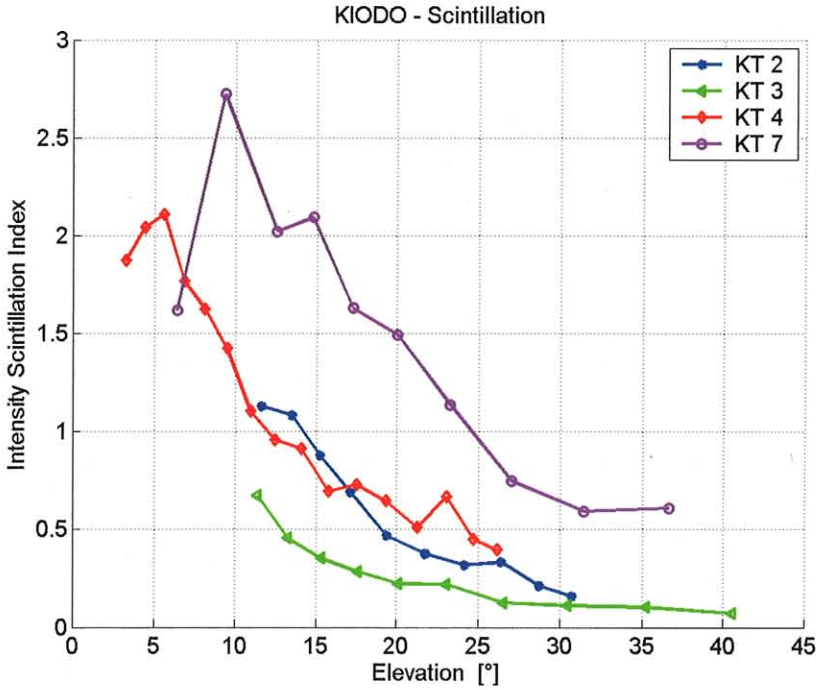

Figure 9.1.1-1 Intensity scintillation index derived from images of the "Profiler" camera.

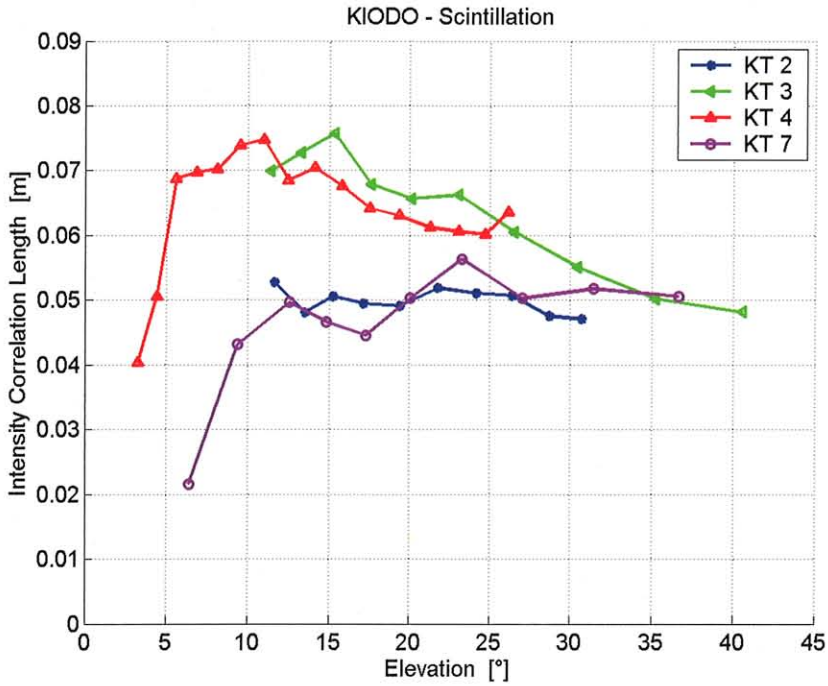

Figure 9.1.1-2 Intensity correlation length derived from images of the "Profiler" camera.

Remark:

For the same elevation, approximately same daytime and location, the scintillation during Trial #7 was about 5 times stronger than the scintillation during Trial #3!

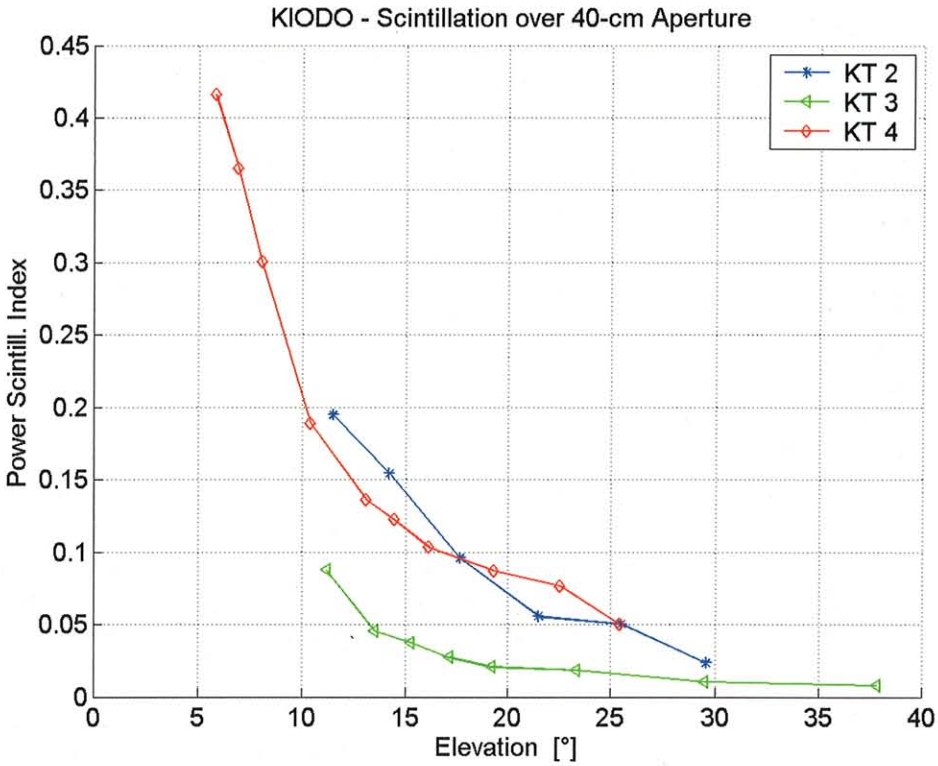

Figure 9.1.1-3 Power scintillation index derived from PIN-diode measurements. The aperture diameter is 40 cm.

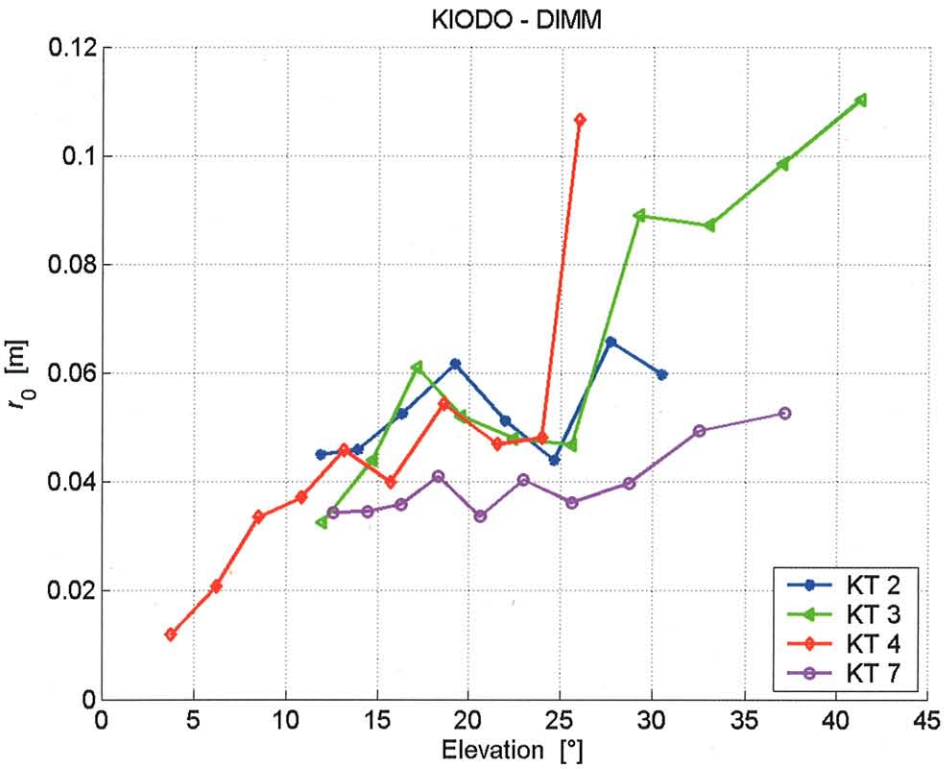

Figure 9.1.1-4 Measurement of the r_0 parameter for all trials.

9.1.2 BER (Summary)

All BER measurements are gathered in Figure 9.1.2-1.

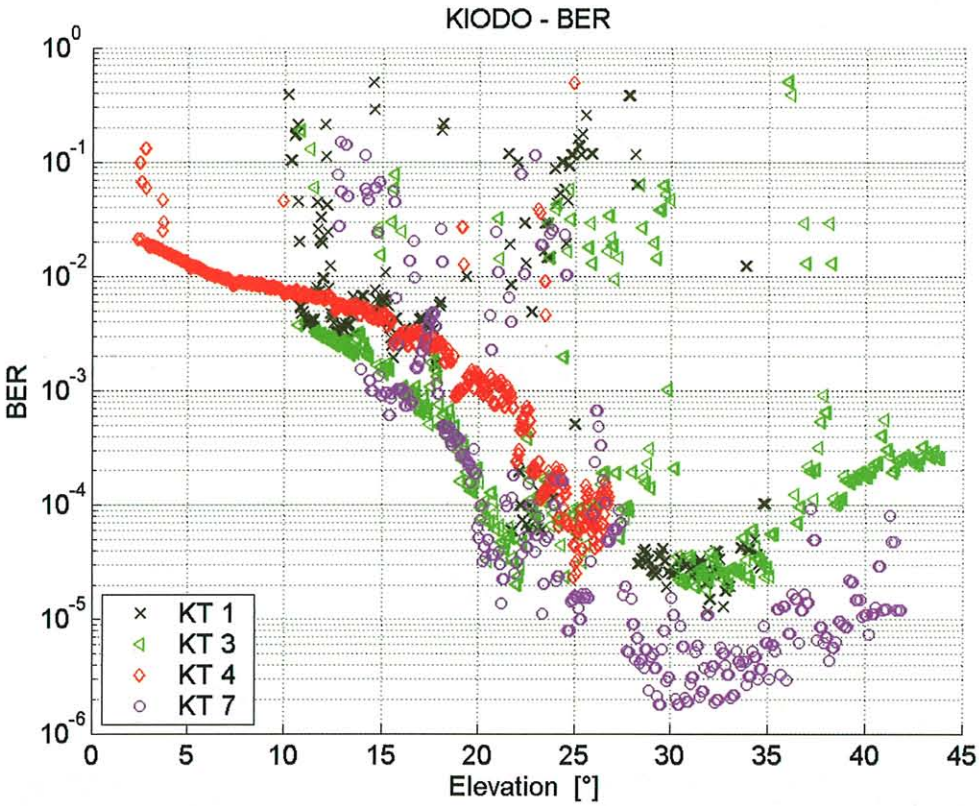

Figure 9.1.2-1 Measured BER (Summary)

9.1.3 Uplink Scintillation (Summary)

All measured intensity scintillation indices for the uplink are gathered in Figure 9.1.3-1. The scintillation of the beacon beam was reduced by transmitting it as a spatially incoherent beam (see Chapter 16 in [AND05]). The spectrograms of associated trials are shown in Figure 9.1.3-2. These spectrograms could be calculated up to 500 Hz only.

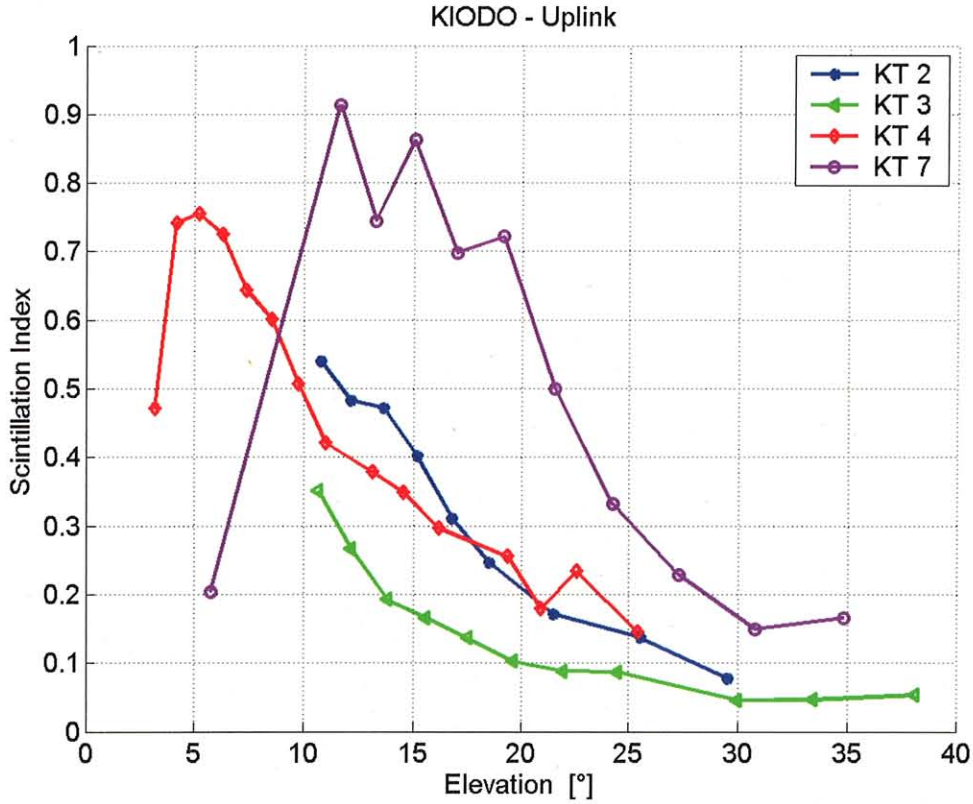

Figure 9.1.3-1 Uplink scintillation indices (Summary)

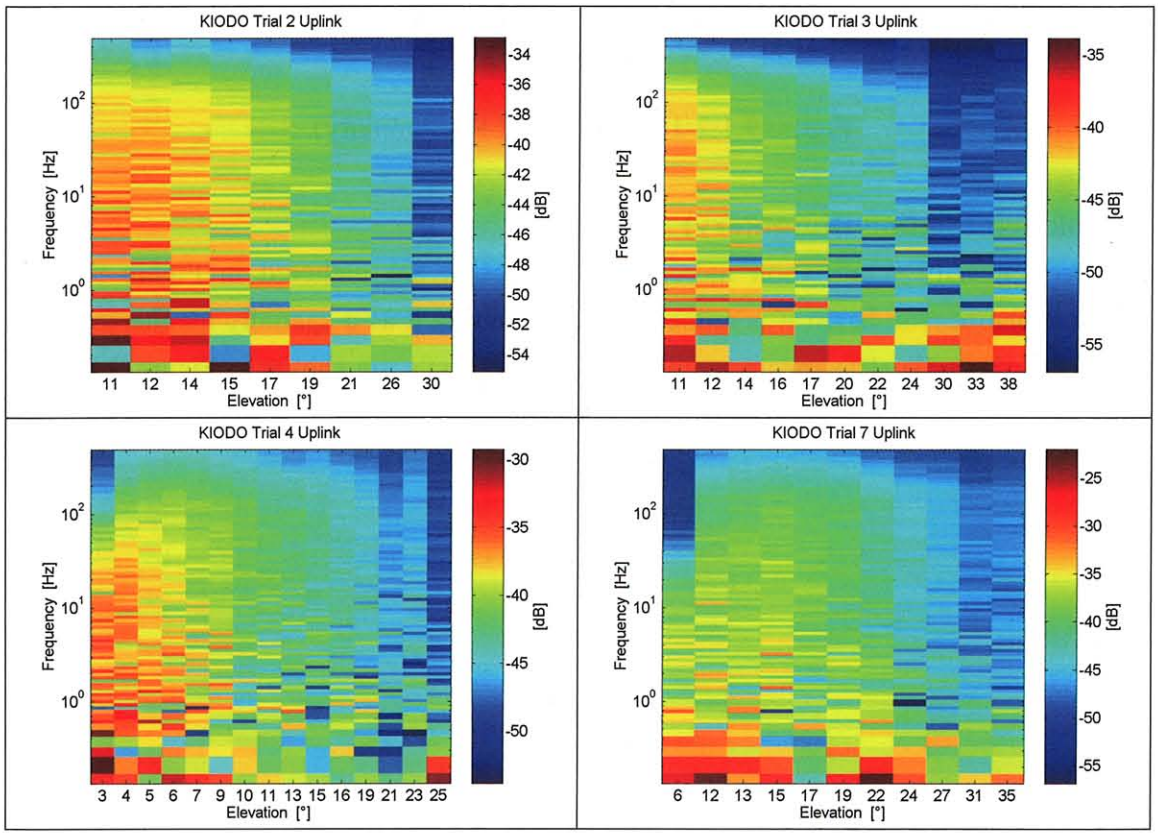

Figure 9.1.3-2 Spectrograms of the uplink power for trials 2, 3, 4, and 7.

9.2 OICETS measurement

9.2.1 Open pointing error

The open pointing errors of LUCE are plotted in Figure 9.2.1-1 with the date of experiment. Figure 9.2.1-2 shows the open pointing errors projected on a plane of the coarse pointing sensor. The dotted circle of the radius 0.2deg. is the field-of-view of the coarse pointing sensor, and the circle of the radius 0.25deg. indicates the marginal area of the coarse pointing sensor. These figures show that LUCE could point the ground station properly in all the KIODO trials.

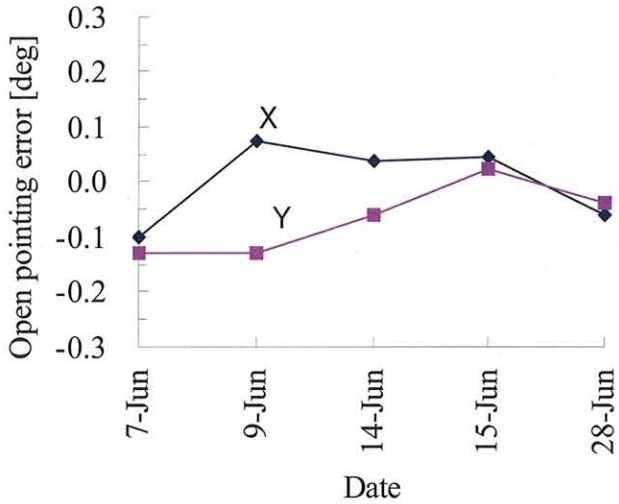

Figure 9.2.1-1 Open pointing error.

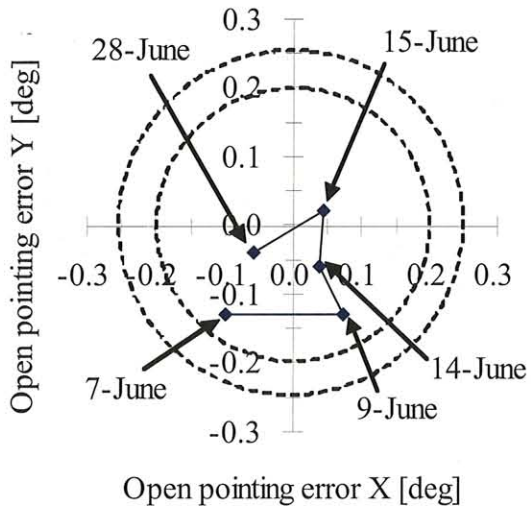

Figure 9.2.1-2 Open pointing error projected on a plane of the coarse pointing sensor.

9.2.2 Measurements

The summary of the OICETS measurement is given in Table 9.2.2-1.

Table 9.2.2-1 Summary of OICETS measurement (1/2)

				7 Jun 2006	9 Jun 2006	14 Jun 2006	15 Jun 2006
				01:13:08 - 01:16:09	00:02:29 - 00:05:38	01:04:46 - 01:07:57	23:51:52 - 23:57:19
conditions	OICETS	Comm beam	power (mW)	100	100	100	100
			moduration	PN	PN	PN	PN
	DLR-OGS	Beacon beam	Wavelength(nm)	809	809	809	809
			Total Power(W) at 90deg elevation	0.30	0.15	0.15	0.15
			Total Power (W) at 10deg elevation	---	---	5.00	5.00
			Divergence angle (mrad, FWHM)	5	5	5	5
			Power percentage for beacons (beacons at 809	50, 50	50, 50	50, 50	50, 50
			Mode of beacon power	adjustable	adjustable	adjustable	adjustable
			Power percentage for instruments(Rx, Tracking, Profiler, DIMM, Power meter)	8 ,23, 23, 23, 23	8, 4, 4, 42, 42	8, 4, 4, 42, 42	≦8, 4, 4, 42, 42
			Exposure of DIMM and Profiler, respectively(μrad)	---	150, 100	150, 100	150, 100
data	OICETS	acquisition	time				
			CP LVL (average)	-83.6	-86.4	-85.8	-86.8
			FP LVL (average)	-58.5	-65.1	-65.4	-67.2
			CP X ERR	---	---	---	---
			CP Y ERR	---	---	---	---
			FP X ERR	±0.2 ～±0.9	±0.3 ～±0.7	±0.3 ～±0.7	±0.4 ～±1.3
			FP Y ERR	±0.2 ～±0.7	±0.4 ～±1.1	±0.3 ～±0.7	±0.5 ～±1.4
			Open pointing error Az (deg)	0.03	0.04	0.02	0.02
			Open pointing error El (deg)	-0.13	-0.01	0.02	0.04
		tracking					
	DLR		receive(dBm)				
			BER	1.0E-05	---	1.0E-05	1.0E-05
	Note	acquisition		CPS detection of beacon: 01:12:48 (20sec earlier) Acqusition time: 218ms	CPS detection of beacon: 00:01:54 (35sec earlier) Acqusition time: 235ms	CPS detection of beacon: 01:04:26 (20sec earlier) Acqusition time: 157ms	CPS detection of beacon: 23:52:14 (22sec earlier). OGS's elevation angle at CPS detection was 1.25 deg. Acqusition time: 722ms
		tracking		tracking error: 0.2 to 0.7μrad FPS receiced level: saturated	tracking error: 0.4 to 1.1μrad FPS receiced level: saturated for 50sec from the beginning of the trial	tracking error: 0.3 to 0.7μrad FPS receiced level: saturated for 20sec from the beginning of the trial	tracking error: 0.5 to 1.4μrad FPS receiced level: saturated for 80sec after 150sec from the beginning of the trial
Wether at DLR				clear sky and thin clouds	alomost clear sky	clear sky	cloudy

Table 9.2.2-1 Summary of OICETS measurement (2/2)

				21 Jun 2006	23 Jun 2006	28 Jun 2006	30 Jun 2006
				00:56:12 - 00:59:42	01:19:17 - 01:24:30	00:45:50 - 00:50:46	01:10:53 - 01:16:14
conditions	OICETS	Comm beam	power (mW)	100	100	100	100
			moduration	PN	PN	PN	PN
	DLR-OGS	Beacon beam	Wavelength(nm)	809	809	809	809
			Total Power(W) at 90deg elevation	0.15	0.15	0.15	0.15
			Total Power (W) at 10deg elevation	5.00	5.00	5.00	5.00
			Divergence angle (mrad, FWHM)	8	5	5	5
			Power percentage for beacons (beacons at 809	50, 50	50, 50	50, 50	50, 50
			Mode of beacon power	adjustable	adjustable	adjustable	adjustable
			Power percentage for instruments(Rx, Tracking, Profiler, DIMM, Power meter)	8, 4, 4, 42, 42	8, 4, 4, 42, 42	8, 4, 4, 42, 42	8, 4, 4, 42, 42
			Exposure of DIMM and Profiler, respectively(μrad)	150, 100	150, 100	150, 100	150, 100
data	OICETS	acquisition	time				
			CP LVL (average)	---	---	-86.9	---
			FP LVL (average)	---	---	-71.0	---
			CP X ERR	---	---	---	---
			CP Y ERR	---	---	---	---
			FP X ERR	---	---	±0.8 ~ ±1.5	---
			FP Y ERR	---	---	±1.0 ~ ±2.5	---
			Open pointing error Az (deg)	---	---	0.06	---
			Open pointing error El (deg)	---	---	-0.08	---
		tracking					
	DLR		receive(dBm)	---	---		---
			BER	---	---	1.0E-06	---
	Note	acquisition		Cancelled	Cancelled	CPS detection of beacon: 00:46:34 Acqusition time: 149ms	Cancelled
		tracking				tracking error: 1.0 to 2.5μrad	
Wether at DLR				cloudy	cloudy and rainy	Thunder clouds 1 hour before experiment	cloudy

9.3 Responses to the objectives

The responses to the objectives are given in Table 9.3-1.

Table 9.3-1 Reponses to the objectives

Objectives	Results
To derive data on the downlink transmission channel under the atmospheric effects.	Done
To obtain criteria for investigating the atmospheric influences.	Done
To measure the received power fluctuations on the uplink and downlink channels.	Done
To measure Bit Error Rate (BER) of the received digital signal on the downlink channel.	Done
To evaluate pointing accuracy of optical terminals.	Done
To evaluate accuracy of acquisition and tracking performance of optical terminals.	Done
To derive data on the downlink transmission channel with high angular velocities in optical terminals' movement under the atmospheric effects.	Done

10 Discussions

10.1 BER Measurement at OGS

The best achieved BER of the KIODO experiment is 2×10^{-6}. This value should have been much lower considering the high level of the received signal power and the relatively low data rate. The Doppler effect was not strong enough to cause an impairment of the receiver and degrade the BER values. It is not clear why the BER slightly decreases above 35° elevation for KT3 and KT7. We believe that some jitter present in the received signal and probably induced by atmospheric turbulence has impaired the communication receiver electronics. OOK communication receivers that are robust against scintillation are currently under investigation at DLR.

10.2 Repeated discontinuance of OICETS tracking

In every trial, the detected power at the OGS showed periodical sudden disappearance of the downlink beam as shown in Figure 10.2-1. The period was about 30s. On the other hand, the abrupt loss of the uplink beam was repeatedly observed with the same period in the output of the LUCE's fine pointing sensor as shown in Fig. 8.2.3-1(f) for example. Furthermore, the repeated variation with the period of about 30s was also found in the coarse pointing errors and the fine pointing errors. The phenomenon caused the discontinuance of the optical link. In the following, the origin of such an undesired phenomenon is described.

Among the several sudden disappearances of light in Figure 10.2-1, we concentrate on the first one observed around 150s in the figure for instance. The corresponding phenomenon occurs around 375s as shown in Figure 10.2-2 (a) of LUCE's fine pointing sensor's output. In this figure, the experiment was conducted between 273s and 454s, and Fig. 8.2.3-1 (f) is involved between 239s and 509s. The period of a sudden decrease in the fine pointing sensor level marked with a blue circle is expanded in Figure 10.2-2 (b), where the low output between 375.4s and 376.2s indicates that no light illuminates the active area of the fine pointing sensor.

The angular error of the fine pointing mechanism is shown in Figures 10.2-3 (a)-(d). The outputs on the fine pointing error are invalid when the fine pointing sensor detects no light. As a result, the fine pointing mirrors became in anomaly operation as shown in Figures10.2-4 (a) and 10.2-4 (b) and cause to remove the downlink beam from the expected direction.

The origin of the lost of light at the fine pointing sensor comes from the large pointing error in the coarse pointing mechanism. The figures 10.2-5 (a) and 10.2-5 (b) are the coarse pointing error x and y, respectively. Several abrupt variations are observed during the experiment period in the coarse pointing error y only. The figures 10.2-6 (a) and 10.2-6 (b) show the gimbal azimuth commanded angle and the measured angle, respectively. Since the actual gimbal's movement reflects the

commanded angles, the cause of the repeated phenomenon is regarded as the gimbal control algorithm. The figure 10.2-7 confirms that the timing of gimbal's abrupt movement corresponds with that of the periodical discontinuance.

The gimbal's velocities in the azimuth and the elevation directions are shown in Table 10.2-1 with the local peak label defined in Figure 10.2-8. Figures 10.2-9 and 10.2-10 plot the local peak values of the coarse pointing sensor Y and the gimbal's velocities, respectively. Those figures clearly indicate that the local peak values of the coarse pointing sensor correlates with the gimbal velocity in the azimuth direction. According to those figures, it is understood that the repeated lost of light detected at the OGS was caused by LUCE's tracking and pointing characteristics.

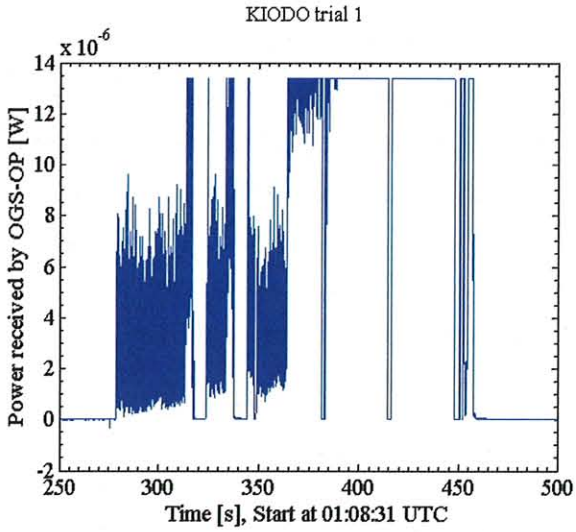

Figure 10.2-1 Detected power at the OGS on 7th June 2006.

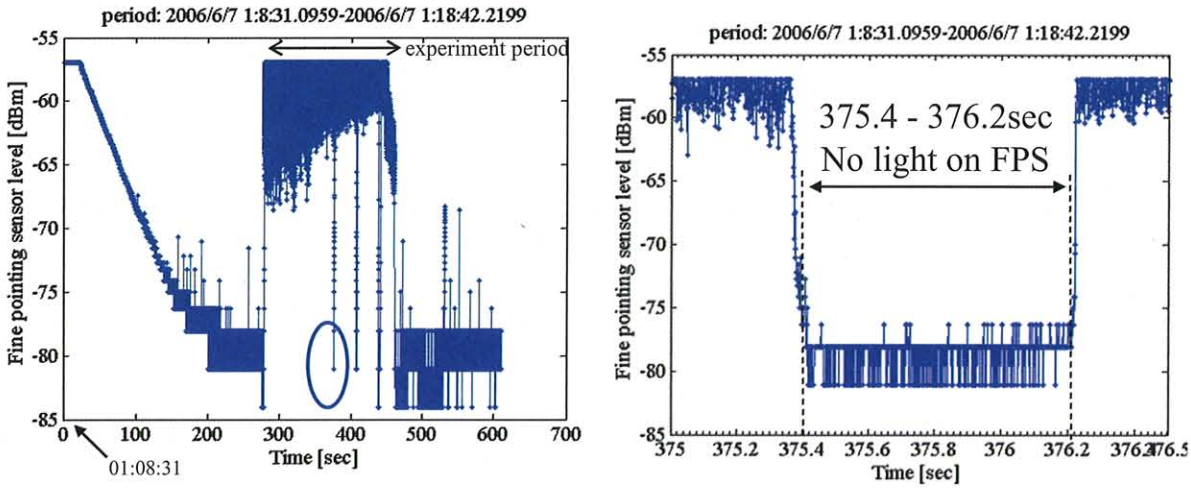

(a) (b)

Figure 10.2-2 (a)LUCE's fine pointing senor output, and (b)partial expansion between 375s and 376.5s

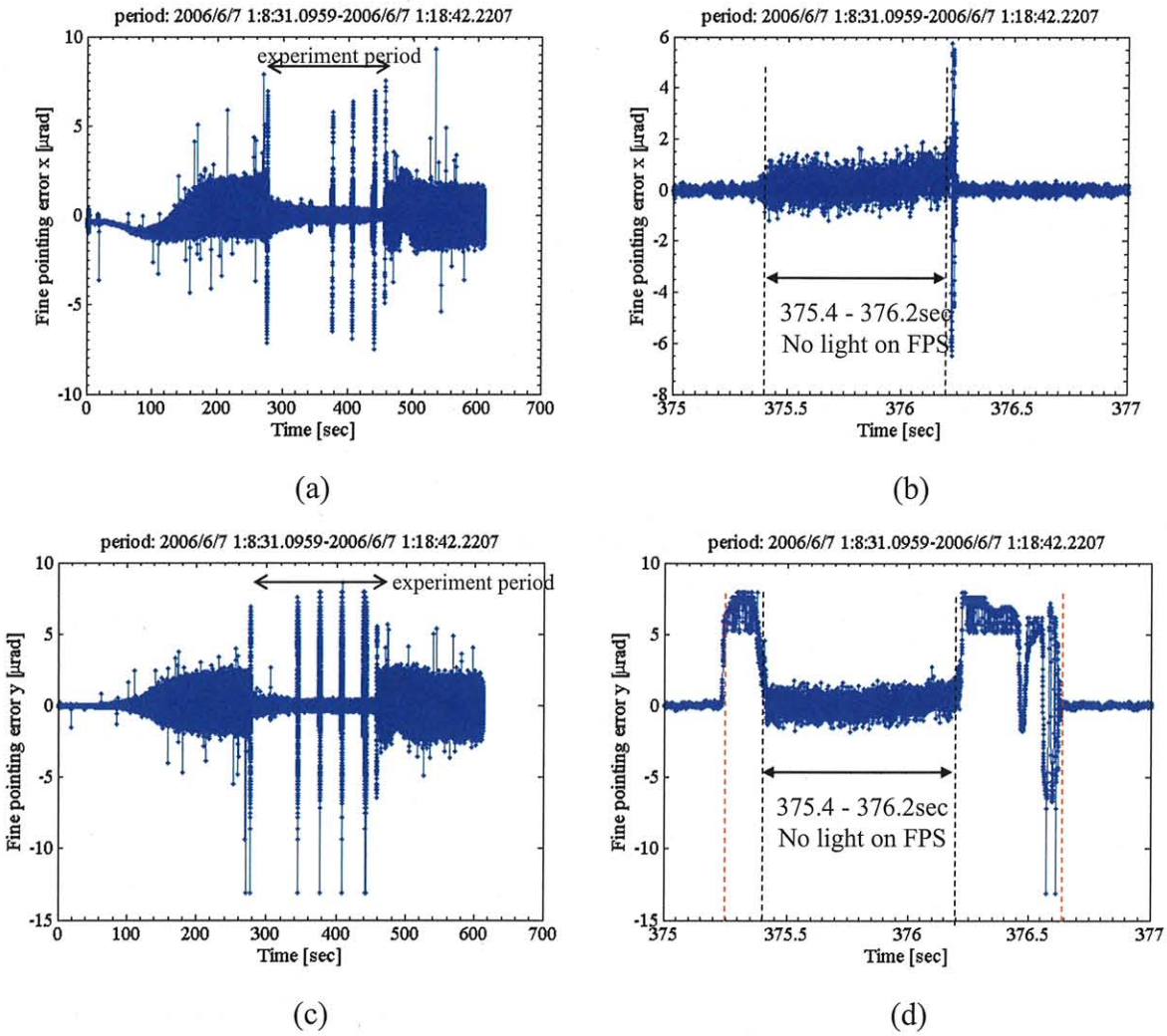

Figure 10.2-3 (a) LUCE's fine pointing error x, (b) partial expansion between 375s and 377s, (c) LUCE's fine pointing error y, and (d) partial expansion between 375s and 377s

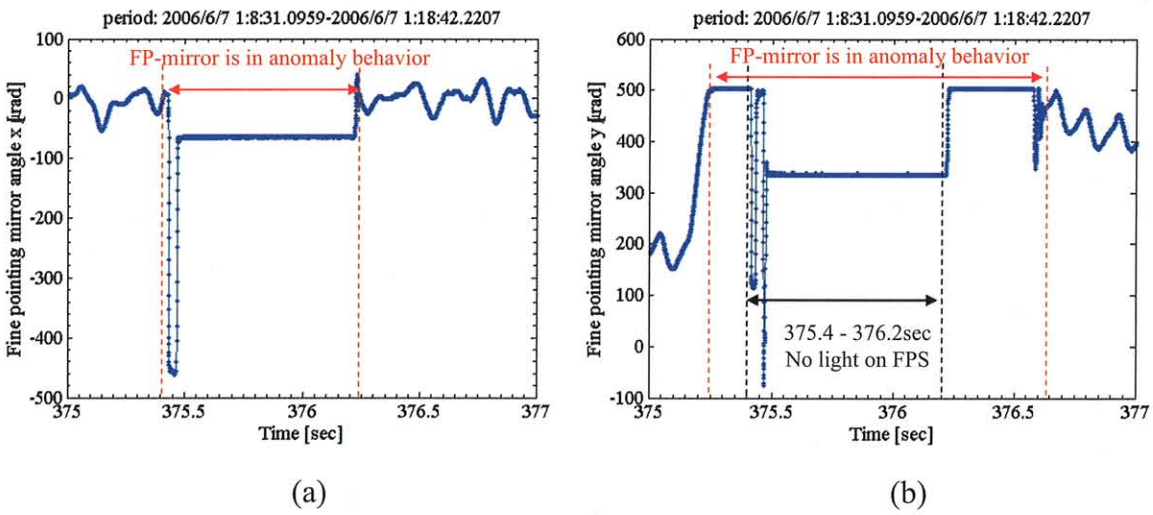

Figure 10.2-4 (a) LUCE's fine pointing mirror angle x, and (b) y

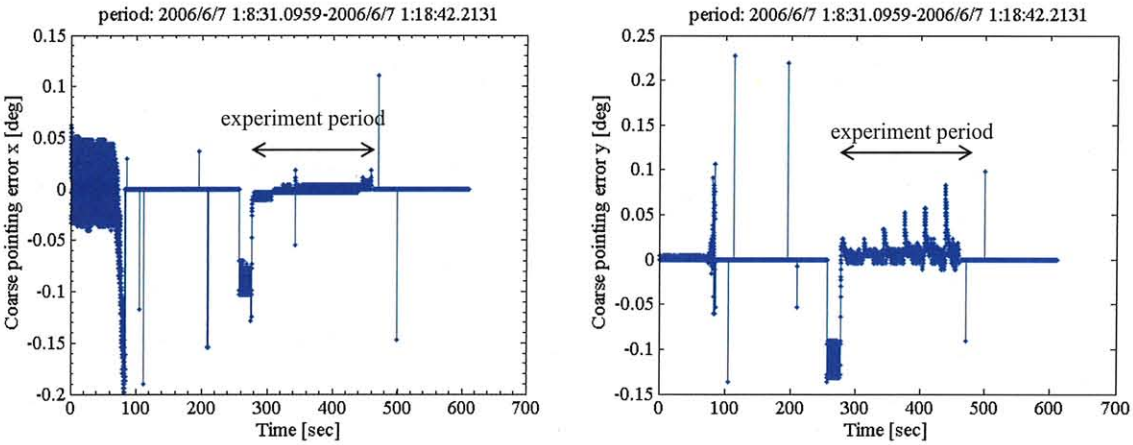

(a) (b)

Figure 10.2-5 Coarse pointing error (a) x, and (b) y

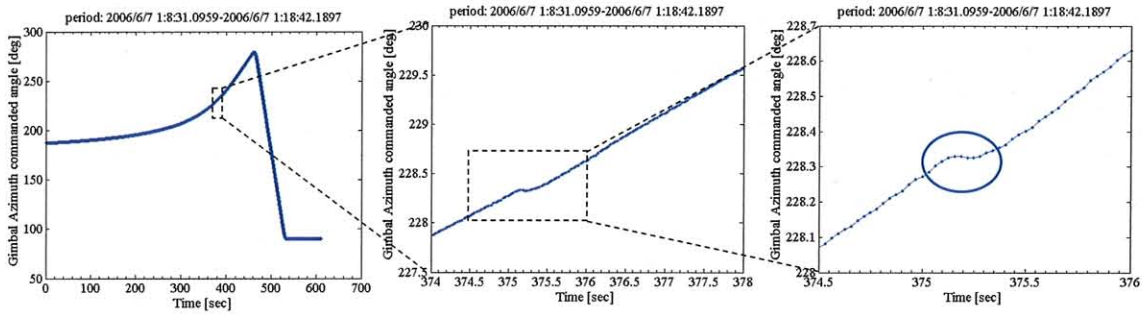

(a)

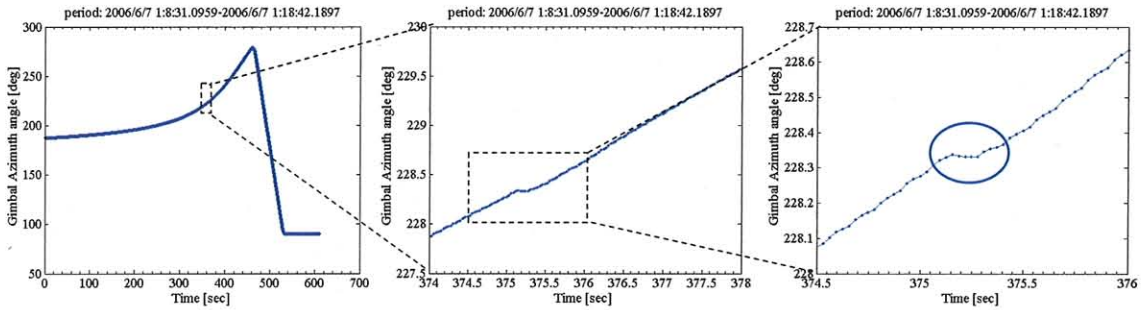

(b)

Figure 10.2-6 Gimbal azimuth (a) commanded angle, and (b) measured angle

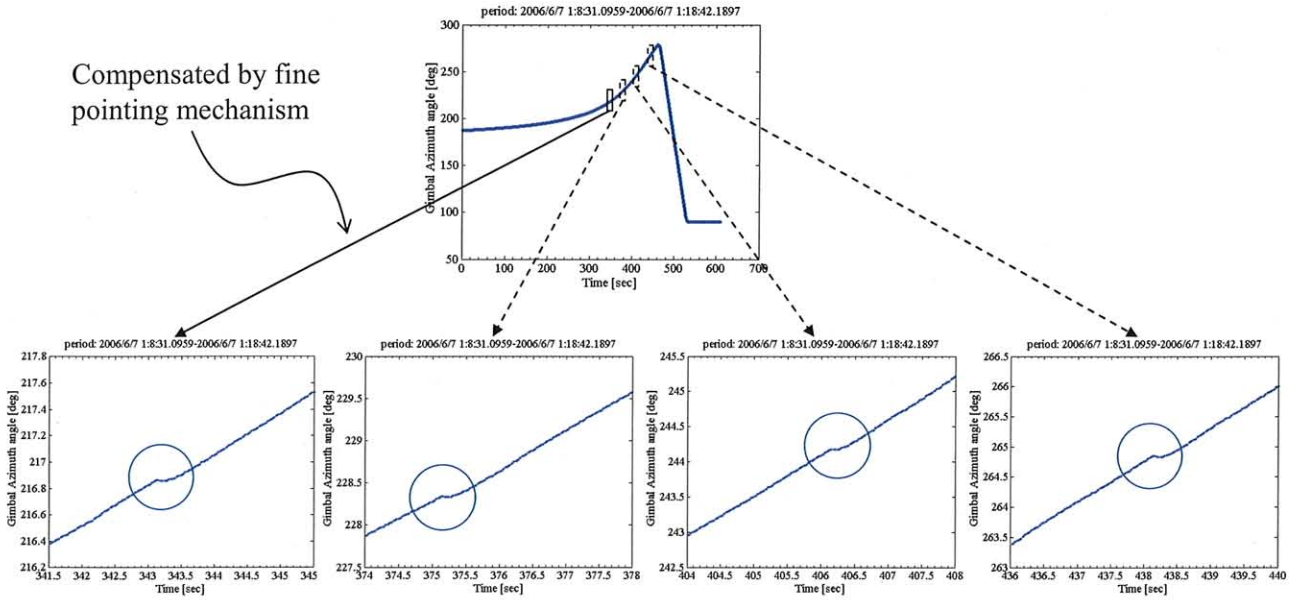

Figure 10.2-7 Periodical abrupt changes in gimbal azimuth angle

Table 10.2-1 Gimbal velocity

Local peak No.	1	2	3	4	5	6
relative time [sec]	281	313	342	376	408	439
CP error y peak [deg]	0.023	0.023	0.034	0.053	0.057	0.083
Azimuth velocity [deg/s]	0.147	0.205	0.291	0.429	0.588	0.678
Elevation velocity [deg/s]	0.078	0.081	0.078	0.057	0.001	0.121

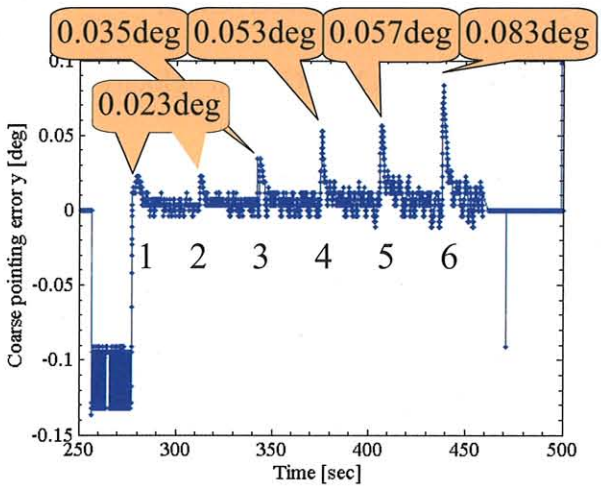

Figure 10.2-8 Label of local peaks

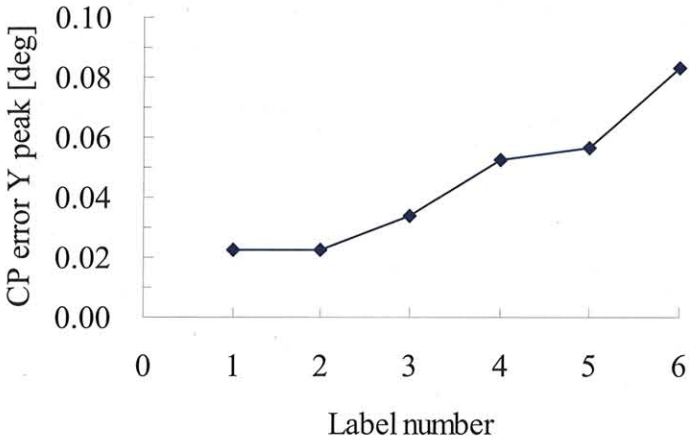

Figure 10.2-9 Local peak values

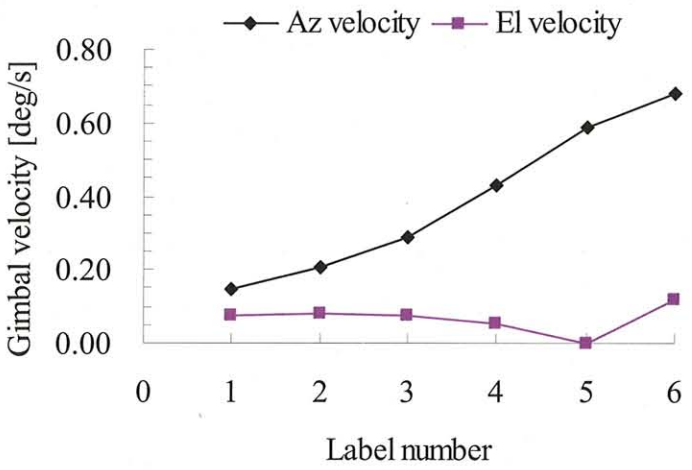

Figure 10.2-10 Gimbal velocity

11 Conclusions

In the cooperative project KIODO, DLR and JAXA successfully executed downlink experiments from OICETS to OGS and demonstrated the feasibility of high-speed optical data downlinks from LEO satellites to simple, inexpensive optical ground terminals for future use. It is believed that, for such a scenario, an error-free data transmission can be achieved with a receiving front-end that is more robust against scintillation. We observed a general agreement of measurements with scintillation theory. Measurements at low elevations have enabled the observation of scintillation saturation. Since the gimbals angular movement required in the ground-satellite demonstration was much faster than that in the inter-orbit communications, LUCE's marginal operation characteristics were observed. This successful experiment encourages to further pursue the concept of direct optical high-speed downlinks from earth observation satellites.

12 Notation

A TV crew was present during KIODO trial #7 and a documentary video in English/German has been produced.

13 Acknowledgements

DLR's optical communication group thanks M. Toyoshima and the optical group of NICT for their help and advices.

JAXA's OICETS project team thanks NEC TOSHIBA Space Systems Ltd., Space Engineering Development Co., Ltd., Fujitsu Ltd., Sorun Co., and Daiko Denshi Tsushin Ltd. for their support to the planning and operation of OICETS satellite and the ground facilities. OICETS project team also appreciates JAXA's flight dynamics facility to create the OICETS orbit information for KIODO demonstrations.

References

[AND05] L. Andrews, R. Phillips, Laser Beam Propagation through Random Media, 2nd Edition, SPIE Press, Bellingham, WA, (2005).

[AUS05] http://www.ga.gov.au/geodesy/datums/cosys.jsp, " Updated: 28 June 2005, Differences between coordinate systems".

[JON06] T. Jono, Y. Takayama, N. Kura, K. Ohinata, Y. Koyama, K. Shiratama, Z. Sodnik, B. Demelenne, A. Bird and K. Arai, "OICETS on-orbit laser communication experiments", Proc. SPIE, 6105, pp. 610503-1-610503-11, 2006.

[MAY02] B. Mayer, S. Shabdanov, D. Giggenbach, "Electronic Database of atmospheric absorption coefficients", DLR-internal report by DLR-IPA and DLR-IKN-DN-OCG, DLR-Oberpfaffenhofen (2002), based on the atmospheric constituents profiles according to "G.P. Anderson, et al: AFGL Atmospheric Constituent Profiles (0-120km), AFGL-TR-86-0110, Hanscom Air Force Base, MA 01736 (1986)"

[PAP91] A. Papoulis, Probability, Random Variables, and Stochastic Processes, 3rd ed. (McGraw-Hill, Inc), 1991.

[PEA02] Pearlman, M.R., Degnan, J.J., and Bosworth, J.M., "The International Laser Ranging Service", Advances in Space Research, Vol. 30, No. 2, pp. 135-143, July 2002.

[PER07] N. Perlot, M. Knapek, D. Giggenbach, J. Horwath, M. Brechtelsbauer, Y. Takayama and T. Jono," Results of the optical downlink experiment KIODO from OICETS satellite to optical ground station Oberpfaffenhofen (OGS-OP)", *Free-Space Laser Communication Technologies XIX, Proc. of SPIE*, 645704 (2007)

[RIC06] R.F.Ricklefs 2006, http://ilrs.gsfc.nasa.gov/docs/cpf_1.01.pdf

[SAR90] M. Sarazin and F. Roddier, "The ESO differential image motion monitor," Astron. Astrophy., 227, 294-300, 1990.

[TOK02] A. Tokovinin, V. Kornilov, "Measuring turbulence profile from scintillations of single stars." In: Astronomical Site Evaluation in the visible and Radio Range, Eds. Benkhaldoun Z., Muñoz-Tuñon C., Vernin J., ASP Conf. Ser., V. 266, p. 104-112, 2002

[TOK02b] A. Tokovinin, "From Differential Image Motion to Seeing", Publications of the Astronomical Society of the Pacific, 114, 1156–1166, 2002.

Participants

DLR:

Brechtelsbauer, M.

Giggenbach, D. (Dr)

Horwath, J.

Knapek, M.

Perlot, N. (Dr)

Contact Person:
nicolas.perlot@dlr.de

JAXA:

Arai, K.

Jono,T.

Koyama, Y.

Kura, N.

Ohinata, K.

Ohshio, K.

Tateshita, Y.

Takayama, Y. (Dr)

Contact Person:
takayama.yoshihisa@jaxa.jp

ISSN 1349-1121
JAXA-RM-07-003E

Printed on Recycled Paper